

Induced gravitational waves: the effect of first order tensor perturbations

Raphaël Picard^a and Karim A. Malik^a

^aQueen Mary University of London, London, E1 4NS, United Kingdom

E-mail: r.h.j.picard@qmul.ac.uk, k.malik@qmul.ac.uk

Abstract. Scalar induced gravitational waves contribute to the cosmological gravitational wave background. They can be related to the primordial density power spectrum produced towards the end of inflation and therefore are a convenient new tool to constrain models of inflation. These waves are sourced by terms quadratic in perturbations and hence appear at second order in cosmological perturbation theory. While the focus of research so far was on purely scalar source terms we also study the effect of including first order tensor perturbations as an additional source. This gives rise to two additional source terms: a term quadratic in the tensor perturbations and a cross term involving mixed scalar and tensor perturbations. We present full analytical expressions for the spectral density of these new source terms and discuss their general behaviour. To illustrate the generation mechanism we study two toy models containing a peak on small scales. For these models we show that the scalar-tensor contribution becomes non-negligible compared to the scalar-scalar contribution on smaller scales. We also consider implications for future gravitational wave surveys.

Contents

1	Introduction	2
2	The second order gravitational wave equation	3
2.1	Extracting gravitational wave source terms	3
2.2	Solving the GW equation	4
3	Extracting the power spectrum	6
3.1	Scalar-scalar power spectrum	7
3.2	Tensor-tensor power spectrum	8
3.3	Scalar-tensor power spectrum	9
4	Results: peaked power spectra	10
4.1	Current energy density of gravitational waves	10
4.1.1	Spectral density of the scalar-scalar contribution	11
4.1.2	Spectral density of the tensor-tensor contribution	11
4.1.3	Spectral density of the scalar-tensor contribution	12
4.2	Comments on potential divergences and resonances	12
4.3	Monochromatic power spectra	13
4.3.1	Peak at the same scale	13
4.3.2	Peaks at a different scale	16
4.4	Lognormal Peak	17
5	Discussion	18
A	Evolution equations	21
A.1	Background equations	21
A.2	First order equations	21
A.3	Second order equations	22
B	Fourier space conventions	22
C	Polarization functions	23
C.1	Convolution symmetry in the tensor-tensor sector	23
C.2	Integral evaluations of the polarization functions	24
D	Evaluation of kernels	25
D.1	Definition of the functions	25
D.2	Kernel results	26

1 Introduction

The first direct detection of gravitational waves by the LIGO/Virgo collaboration [1], resulting from the merger of two black holes, and subsequent detections, reignited cosmologists interests in using gravitational waves as a novel probe into the early universe. Recently, thanks to cosmic timing arrays, the NANOGrav collaboration [2], the EPTA/InPTA [3–5], the CPTA [6] and the PPTA [7, 8] published data that provides evidence for a low frequency stochastic gravitational wave background (SGWB). Although the source of the SGWB is as yet undetermined, this evidently is a milestone for researchers who have predicted a SGWB of cosmological origin. The NANOGrav collaboration also fitted cosmological sources [9] such as domain walls, cosmic strings and cosmological phase transitions to their data release, but stress that their results should not (yet) be taken as evidence for new physics.

On the theory side, inflation allows for two different and independent ways of production of gravitational waves, leading to different observational signatures. At linear order, gravitational waves produced during inflation have been studied for some time now and have become a well established tool to discriminate between models of inflation [10]. They can leave a distinct imprint in the Cosmic Microwave Background (CMB) in form of B-mode polarisation. For example, the Planck collaboration has extracted an upper limit on the tensor-to-scalar ratio $r < 0.065$, at $k = 0.002 \text{ Mpc}^{-1}$ [12]. Going beyond linear order in perturbation theory allows us to study scalar induced gravitational waves (SIGWs), which are gravitational waves that are sourced by terms quadratic in linear order scalar quantities. SIGWs were first studied in the 1960's by K. Tomita [11] and later on by Refs. [13–17], amongst others. Unlike first order gravitational waves, they have a non-negligible source term which is related to the primordial scalar power spectrum. These fluctuations couple to produce gravitational waves. The Planck collaboration determined the scalar power spectrum and gives the value of the spectral index $n_s = 0.9626 \pm 0.0057$ at $k = 0.05 \text{ Mpc}^{-1}$ [12].

In order for SIGWs to be detectable there needs to be some enhancement of the scalar power spectrum (see e.g. Ref. [18] for a review). Both the parameters r and n_s are constrained at CMB scales, and *a priori* there is no reason that these values hold for scales that exit the horizon in the last stages of inflation. There are multiple ways to enhance the primordial scalar power spectrum: for example in single field inflation via a period of ultra-slow-roll [21–24] or in multi-field models of inflation [25–27]. The basic idea is that the power spectrum of SIGWs (\mathcal{P}_{SS}) is related to the linear power spectrum, \mathcal{P}_ζ , as: $\mathcal{P}_{SS} \propto \mathcal{P}_\zeta^2$, so that if there is an enhancement/peak in \mathcal{P}_ζ there will also be one in \mathcal{P}_{SS} . Depending on the scale at which this enhancement happens, the resulting background of gravitational waves can be in principle observable by future detectors such as the Laser Interferometer Space Antenna (LISA) [31], DECi-hertz Interferometer Gravitational wave Observatory (DECIGO) [32] and the Einstein Telescope (ET) [33] to name a few.

Most recent research has been centered around how scalar fluctuations couple to produce SIGWs. However, there is also the possibility that a scalar fluctuation couples with a tensor mode or that two tensor modes couple to induce more general second order gravitational waves (SOGWs). Moreover, if there is also a peak (on smaller scales) of primordial gravitational waves, then we could expect to see its imprint also at second order. Multifield models of inflation can produce such a peak, for example models containing a spectator axion coupled to a $SU(2)$ gauge field [28–30]. This was looked at in Ref. [20] for monochromatic power spectra and in Ref. [36] analytical expressions for the kernels are derived. Recently, Ref. [37] studied scalar-tensor induced gravitational waves in a radiation dominated universe with a

possibility of having an initial parity violation and Ref. [38] looked at the case where the primordial power spectrum follows a sudden-broken power-law.

In this paper we look at the production of SOGWs in a homogeneous and isotropic universe sourced by first order scalar and tensor modes. We will derive the power spectrum of SOGWs $\mathcal{P}_{h^{(2)}}(\eta, k)$ defined as

$$\langle h_{\lambda}^{(2)}(\eta, \mathbf{k}) h_{\lambda'}^{(2)}(\eta, \mathbf{k}') \rangle = \delta^{(3)}(\mathbf{k} + \mathbf{k}') \delta^{\lambda\lambda'} \frac{2\pi^2}{k^3} \mathcal{P}_{h^{(2)}}(\eta, k) , \quad (1.1)$$

where $\lambda, \lambda' = +, \times$ are the polarization states of the GWs. We will use the fact that the spectrum can be decomposed into the sum of the independent contributions of the scalar-scalar, tensor-tensor (\mathcal{P}_{tt}) and scalar-tensor induced waves (\mathcal{P}_{st}) power spectra, such that:

$$\mathcal{P}_{h^{(2)}}(\eta, k) = \mathcal{P}_{ss}(\eta, k) + \mathcal{P}_{tt}(\eta, k) + \mathcal{P}_{st}(\eta, k) . \quad (1.2)$$

Assuming there is a peaked power spectrum for both first the order power spectrum of scalars and tensors, we will parameterise them by four parameters: \mathcal{A}_{ζ} , the amplitude of the scalar power spectrum, k_{ζ} , the scale at which the scalar power spectrum peaks), \mathcal{A}_h , the amplitude of the tensor power spectrum and k_h the scale at which the tensor power spectrum peaks. Given these parameters we will show that there is a non-negligible contribution from considering tensors as an additional source term. Our results include the density of SOGWs and expressions for their corresponding kernels.

We begin in Section 2 by investigating what terms source gravitational waves and solve the equation of motion for these induced tensor modes. Section 3 shows how to obtain the power spectrum of SOGWs, followed by Section 4 where we derive expressions for the spectral density and plot the latter for peaked power spectras. We use the ‘mostly plus’ metric, Greek indices run over from 0, 1, 2, 3, whilst Latin indices run over the spatial coordinates 1, 2, 3 and we work in natural units, i.e. $c = 1$, and define $M_{Pl}^2 = (8\pi G)^{-1}$.

2 The second order gravitational wave equation

2.1 Extracting gravitational wave source terms

We use the conformal Newtonian gauge in a flat FLRW background, see e.g. Ref. [42] for a review of cosmological perturbation theory. We do not include vectors at any order since they are diluted away during inflation. The line element is given by [39]

$$ds^2 = a^2(\eta) \left[-(1 + 2\Phi + \Phi^{(2)})d\eta^2 + \left((1 - 2\Psi - \Psi^{(2)})\delta_{ij} + 2\bar{h}_{ij} + \bar{h}_{ij}^{(2)} \right) dx^i dx^j \right] , \quad (2.1)$$

where η is conformal time, $a(\eta)$ the conformal scale factor and δ_{ij} is the Kronecker delta. Metric perturbations $\Phi^{(n)}, \Psi^{(n)}$ are respectively the lapse and curvature perturbations and $\bar{h}_{ij}^{(n)}$ are tensorial perturbations, which are transverse-traceless (TT): $\partial^i \bar{h}_{ij}^{(n)} = \delta^{ij} \bar{h}_{ij}^{(n)} = 0$. Here (n) is the perturbative order. Additionally, to reduce clutter, we have taken the convention to only show the order of perturbation for second order variables and get rid of the overline which indicates when a tensorial quantity is TT.

We are interested in the second order equation of motion for tensors, therefore only TT tensorial quantities will contribute. We can extract TT quantities by applying the TT

projection operator Λ_{ab}^{ij} to the Einstein equations at second order. This operator can be defined in the following way, see Ref. [19],

$$\Lambda_{ab}^{ij} = \left(\delta_a^i - \frac{\partial^i \partial_a}{\nabla^2} \right) \left(\delta_b^j - \frac{\partial^j \partial_b}{\nabla^2} \right) - \frac{1}{2} \left(\delta_{ab} - \frac{\partial_a \partial_b}{\nabla^2} \right) \left(\delta^{ij} - \frac{\partial^i \partial^j}{\nabla^2} \right), \quad (2.2)$$

where the inverse Laplacian defined by its action on the Laplacian of a tensor field X as: $\nabla^{-2}(\nabla^2 X) = X$. The second order Einstein equations can be found in App. A.3. Hence, in real space we find

$$\Lambda_{ab}^{ij} G_{ij}^{(2)} = \frac{1}{M_{Pl}^2} \Lambda_{ab}^{ij} T_{ij}^{(2)}. \quad (2.3)$$

We study SOGWs sourced by modes produced during inflation and re-entering during the radiation dominated (RD) epoch, and describe the energy content of the universe as an adiabatic perfect fluid with energy momentum-tensor

$$T_{\mu\nu} = (\rho + P)u_\mu u_\nu + P g_{\mu\nu}, \quad (2.4)$$

where ρ and P are, respectively, the energy density and pressure, and u^μ the 4-velocity. Throughout this paper we neglect anisotropic stress, as it has been shown to have a negligible effect on the spectrum of SIGWs [17]. Then Eq. (2.3) becomes:

$$h_{ab}''^{(2)} + 2\mathcal{H}h_{ab}'^{(2)} - \nabla^2 h_{ab}^{(2)} = S_{ab}, \quad (2.5)$$

where S_{ab} is the source term. We separate the source term into quadratic pure first order scalar contributions (ss), quadratic pure first order tensor contributions (tt) and a scalar-tensor cross term (st), such that:

$$S_{ab} = S_{ab}^{ss} + S_{ab}^{tt} + S_{ab}^{st}. \quad (2.6)$$

These terms are given by:

$$S_{ab}^{ss} = \frac{8}{3(1+w)} \left[(\partial_a \Psi + \frac{\partial_a \Psi'}{\mathcal{H}})(\partial_b \Psi + \frac{\partial_b \Psi'}{\mathcal{H}}) \right] + 4\partial_a \Psi \partial_b \Psi, \quad (2.7a)$$

$$S_{ab}^{tt} = -4h^{cd} \partial_c \partial_d h_{ab} + 4\partial_d h_{bc} \partial^c h_a^d - 4\partial_d h_{bc} \partial^d h_a^c + 8h^{dc} \partial_a \partial_c h_{bd} + 4h_a^c h_{bc}' + 2\partial_a h^{cd} \partial_b h_{cd}, \quad (2.7b)$$

$$S_{ab}^{st} = 8\Psi \nabla^2 h_{ab} + 8\partial_c h_{ab} \partial^c \Psi + 4h_{ab} (\mathcal{H}(1 + 3c_s^2) \Psi' + (1 - c_s^2) \nabla^2 \Psi). \quad (2.7c)$$

Note that these expressions have been simplified using first order equations of motion, which can be found in App. A.2. Now that we have extracted the source terms we can move on to solving Eq. (2.5), which we will do in the next section.

2.2 Solving the GW equation

It is convenient to solve this equation in Fourier space, see App. B for conventions. For each polarization $\lambda = +, \times$, Eq. (2.5) turns into

$$h_\lambda^{(2)''}(\eta, \mathbf{k}) + 2\mathcal{H}h_\lambda^{(2)'}(\eta, \mathbf{k}) + k^2 h_\lambda^{(2)}(\eta, \mathbf{k}) = 4S_\lambda(\eta, \mathbf{k}), \quad (2.8)$$

with $S_\lambda(\eta, \mathbf{k}) = S_\lambda^{ss}(\eta, \mathbf{k}) + S_\lambda^{tt}(\eta, \mathbf{k}) + S_\lambda^{st}(\eta, \mathbf{k})$. To solve the above, we use Green's method:

$$h_\lambda^{(2)}(\eta, \mathbf{k}) = \frac{4}{a(\eta)} \int^\eta d\bar{\eta} G_{\mathbf{k}}(\eta, \bar{\eta}) a(\bar{\eta}) S_\lambda(\bar{\eta}, \mathbf{k}), \quad (2.9)$$

where $G_{\mathbf{k}}(\eta, \bar{\eta})$ solves:

$$G_{\mathbf{k}}''(\eta, \bar{\eta}) + 2\mathcal{H}G_{\mathbf{k}}'(\eta, \bar{\eta}) + k^2 G_{\mathbf{k}}(\eta, \bar{\eta}) = \delta(\eta - \bar{\eta}) . \quad (2.10)$$

In our work we look at modes which re-enter the horizon and interact during RD, hence $\mathcal{H} = 1/\eta$, which leads to:

$$G_{\mathbf{k}}(\eta, \bar{\eta}) = \frac{1}{k} \sin(k\eta - k\bar{\eta}) . \quad (2.11)$$

The solution of Eq. (2.9) depends on the evolution of the first order scalar and tensor modes. When these modes are super-Hubble their amplitudes are constant (i.e. when $k\eta < 1$) and set during inflation. This implies we can split their respective equations of motion as a combination of its primordial value and a transfer function. For the first order scalar modes we define

$$\Psi(\eta, \mathbf{k}) = \Psi_{\mathbf{k}} \frac{3}{(c_s x)^2} \left(\frac{\sin c_s x}{c_s x} - \cos c_s x \right) \equiv \frac{2}{3} \zeta_{\mathbf{q}} T_{\Psi}(c_s x) , \quad (2.12)$$

where ζ is the comoving curvature perturbation conserved when the mode is super-Hubble. For the first order tensor modes:

$$h^{\lambda}(\eta, \mathbf{q}) = h_{\mathbf{k}}^{\lambda} \frac{\sin x}{x} \equiv h_{\mathbf{k}}^{\lambda} T_h(x) , \quad (2.13)$$

where we have defined $x = k\eta$ in order to solve Eq. (A.6) and Eq. (A.8) in Fourier space. Both transfer functions are symmetric $\mathbf{k} \rightarrow -\mathbf{k}$.

Finally, splitting the contributions to Eq. (2.9) into pure scalar, tensor and mixed we arrive at using Eqs. (2.7), (2.12) and (2.13):

$$h_{\lambda,ss}^{(2)} = \frac{16}{9} \int \frac{d^3 \mathbf{p}}{(2\pi)^{\frac{3}{2}}} q^{\lambda,ss}(\mathbf{k}, \mathbf{p}) \zeta_{\mathbf{p}} \zeta_{\mathbf{k}-\mathbf{p}} \int_0^{\eta} d\bar{\eta} \frac{a(\bar{\eta})}{a(\eta)} G_{\mathbf{k}}(\eta, \bar{\eta}) f^{ss}(c_s \bar{\eta} p, c_s \bar{\eta} |\mathbf{k} - \mathbf{p}|) , \quad (2.14a)$$

$$\begin{aligned} h_{\lambda,tt}^{(2)} &= 4 \int \frac{d^3 \mathbf{p}}{(2\pi)^{\frac{3}{2}}} q_1^{\lambda,tt}(\mathbf{k}, \mathbf{p}) h_{\mathbf{p}}^{\lambda_1} h_{\mathbf{k}-\mathbf{p}}^{\lambda_2} \int_0^{\eta} d\bar{\eta} \frac{a(\bar{\eta})}{a(\eta)} G_{\mathbf{k}}(\eta, \bar{\eta}) f_1^{tt}(\bar{\eta} p, \bar{\eta} |\mathbf{k} - \mathbf{p}|) \\ &+ 4 \int \frac{d^3 \mathbf{p}}{(2\pi)^{\frac{3}{2}}} q_2^{\lambda,tt}(\mathbf{k}, \mathbf{p}) h_{\mathbf{p}}^{\lambda_1} h_{\mathbf{k}-\mathbf{p}}^{\lambda_2} \int_0^{\eta} d\bar{\eta} \frac{a(\bar{\eta})}{a(\eta)} G_{\mathbf{k}}(\eta, \bar{\eta}) f_2^{tt}(\bar{\eta} p, \bar{\eta} |\mathbf{k} - \mathbf{p}|) , \end{aligned} \quad (2.14b)$$

$$h_{\lambda,st}^{(2)} = \frac{8}{3} \int \frac{d^3 \mathbf{p}}{(2\pi)^{\frac{3}{2}}} q^{\lambda,st}(\mathbf{k}, \mathbf{p}) h_{\mathbf{p}}^{\lambda_3} \zeta_{\mathbf{k}-\mathbf{p}} \int_0^{\eta} d\bar{\eta} \frac{a(\bar{\eta})}{a(\eta)} G_{\mathbf{k}}(\eta, \bar{\eta}) f^{st}(\bar{\eta} p, c_s \bar{\eta} |\mathbf{k} - \mathbf{p}|) . \quad (2.14c)$$

Note that there is an implicit sum over $\lambda_1, \lambda_2, \lambda_3 = +, \times$ (i.e. for each first order gravitational wave source terms there is a sum over the two polarizations). Each contribution (scalar-scalar, tensor-tensor and scalar-tensor) has been split into three separate parts: First, the functions $q^{\lambda}(\mathbf{k}, \mathbf{p})$ encoding the polarization, shown below:

$$q^{\lambda,ss}(k, p) = q_{\lambda}^{ab}(\mathbf{k}) p_a p_b , \quad (2.15a)$$

$$\begin{aligned} q_1^{\lambda,tt}(k, p) &= q_{\lambda}^{ab}(\mathbf{k}) \left(q_{ab}^{\lambda_2}(\mathbf{p}) q_{\lambda_1}^{cd}(\mathbf{k} - \mathbf{p}) p_c p_d - q_{bc}^{\lambda_1}(\mathbf{k} - \mathbf{p}) q_{a,\lambda_2}^d(\mathbf{p}) (k - p)_d p^c \right. \\ &+ q_{bc}^{\lambda_1}(\mathbf{k} - \mathbf{p}) q_{a,\lambda_2}^c(\mathbf{p}) (k - p)_d p^d - 2q_{\lambda_1}^{dc}(\mathbf{k} - \mathbf{p}) q_{bd}^{\lambda_2}(\mathbf{p}) p_a p_c \\ &\left. - \frac{1}{2} q_{\lambda_1}^{cd}(\mathbf{k} - \mathbf{p}) q_{cd}^{\lambda_2}(\mathbf{p}) (k - p)_a p_b \right) , \end{aligned} \quad (2.15b)$$

$$q_2^{\lambda,tt}(k, p) = q_{\lambda}^{ab}(\mathbf{k}) q_a^{c,\lambda_1}(\mathbf{k} - \mathbf{p}) q_{bc}^{\lambda_2}(\mathbf{p}) . \quad (2.15c)$$

$$q^{\lambda,st}(k, p) = q_{\lambda}^{ab}(\mathbf{k}) q_{ab}^{\lambda_3}(\mathbf{p}) . \quad (2.15d)$$

The second part is the primordial values of the perturbations ζ and h^λ . The third part of Eq. (2.14) is an integral over the retarded time $\bar{\eta}$ of the Green's and transfer functions which describes how modes behave once they re-enter the horizon:

$$f^{ss}(c_s\eta p, c_s\eta|\mathbf{k}-\mathbf{p}|) = \frac{2}{3(1+w)} \left[\left((T_\Psi(c_s\eta|\mathbf{k}-\mathbf{p}|) + \frac{T'_\Psi(c_s\eta|\mathbf{k}-\mathbf{p}|)}{\mathcal{H}}) \left(T_\Psi(c_s\eta p) + \frac{T'_\Psi(c_s\eta p)}{\mathcal{H}} \right) \right) + T_\Psi(c_s\eta|\mathbf{k}-\mathbf{p}|)T_\Psi(c_s\eta p) \right], \quad (2.16a)$$

$$f_1^{tt}(\eta p, \eta|\mathbf{k}-\mathbf{p}|) = T_h(\eta|\mathbf{k}-\mathbf{p}|)T_h(\eta p), \quad (2.16b)$$

$$f_2^{tt}(\eta p, \eta|\mathbf{k}-\mathbf{p}|) = T'_h(\eta|\mathbf{k}-\mathbf{p}|)T'_h(\eta p), \quad (2.16c)$$

$$f^{st}(\eta p, c_s\eta|\mathbf{k}-\mathbf{p}|) = -2p^2T_h(\eta p)T_\Psi(c_s\eta|\mathbf{k}-\mathbf{p}|) - 2(k-p)pT_h(\eta p)T_\Psi(c_s\eta|\mathbf{k}-\mathbf{p}|) + \mathcal{H}(1+3c_s^2)T_h(\eta p)T'_\Psi(c_s\eta|\mathbf{k}-\mathbf{p}|) - (k-p)^2(1-c_s^2)T_h(\eta p) \times T_\Psi(c_s\eta|\mathbf{k}-\mathbf{p}|). \quad (2.16d)$$

Note that the source terms in Fourier space are given by a convolution of the first order perturbations, hence there is a freedom in relabelling (i.e. a symmetry between) $\mathbf{p} \leftrightarrow \mathbf{k}-\mathbf{p}$. This symmetry will be used to simplify calculations when considering the two-point correlation function of $h_\lambda^{(2)}$, in the following section.

3 Extracting the power spectrum

To extract the power spectrum we substitute Eq. (2.9) into the left-hand side of Eq. (1.1). By factorizing out each terms primordial value in Eq. (2.14), it becomes more apparent what contributes to the final power spectrum:

$$h_{ss}^{\lambda(2)}(\eta, \mathbf{k}) = \frac{16}{9k^2} \int \frac{d^3\mathbf{p}}{(2\pi)^{\frac{3}{2}}} q^{\lambda,ss}(k, p) \mathcal{I}_{ss} \zeta_{\mathbf{p}} \zeta_{\mathbf{k}-\mathbf{p}}, \quad (3.1a)$$

$$h_{tt}^{\lambda(2)}(\eta, \mathbf{k}) = \frac{4}{k^3\eta} \int \frac{d^3\mathbf{p}}{(2\pi)^{\frac{3}{2}}} \left(q_1^{\lambda,tt}(k, p) \mathcal{I}_{tt,1} + q_2^{\lambda,tt}(k, p) \mathcal{I}_{tt,2} \right) h_{\mathbf{p}}^{\lambda_1} h_{\mathbf{k}-\mathbf{p}}^{\lambda_2}, \quad (3.1b)$$

$$h_{st}^{\lambda(2)}(\eta, \mathbf{k}) = \frac{8}{3k^3\eta} \int \frac{d^3\mathbf{p}}{(2\pi)^{\frac{3}{2}}} q^{\lambda,st}(k, p) \mathcal{I}_{st} h_{\mathbf{p}}^{\lambda_3} \zeta_{\mathbf{k}-\mathbf{p}}. \quad (3.1c)$$

The tensor-tensor contribution has two terms due to the nature of the polarization functions Eq. (2.15b) and Eq. (2.15c), which means we can't factor out a common factor. In the above we introduced the kernels, $\mathcal{I} \equiv (x, p, |\mathbf{k}-\mathbf{p}|)$, defined as:

$$\mathcal{I}_{ss}(x, p, |\mathbf{k}-\mathbf{p}|) = \int_0^x d\bar{x} f^{ss}(c_s\bar{\eta}p, c_s\bar{\eta}|\mathbf{k}-\mathbf{p}|) \frac{\bar{x}}{x} \sin(x-\bar{x}), \quad (3.2a)$$

$$\mathcal{I}_{tt,1}(x, p, |\mathbf{k}-\mathbf{p}|) = \int_0^x d\bar{x} f_1^{tt}(\bar{\eta}p, \bar{\eta}|\mathbf{k}-\mathbf{p}|) \bar{x} \sin(x-\bar{x}), \quad (3.2b)$$

$$\mathcal{I}_{tt,2}(x, p, |\mathbf{k}-\mathbf{p}|) = \int_0^x d\bar{x} f_2^{tt}(\bar{\eta}p, \bar{\eta}|\mathbf{k}-\mathbf{p}|) \bar{x} \sin(x-\bar{x}), \quad (3.2c)$$

$$\mathcal{I}_{st}(x, p, |\mathbf{k}-\mathbf{p}|) = \int_0^x d\bar{x} f^{st}(\bar{\eta}p, c_s\bar{\eta}|\mathbf{k}-\mathbf{p}|) \bar{x} \sin(x-\bar{x}), \quad (3.2d)$$

where $\bar{x} = k\bar{\eta}$. We note that the pure scalar Kernel has been defined in this particular way in order to use the results from Ref. [41].

Using Wick's theorem and assuming total gaussianity of the linear order perturbations, the two point function reduces to the sum of the three individual contributions¹ (scalar-scalar, tensor-tensor and scalar-tensor):

$$\begin{aligned} \langle h^{\lambda(2)}(\eta, \mathbf{k}) h^{\lambda'(2)}(\eta, \mathbf{k}') \rangle &= \langle h_{ss}^{\lambda(2)}(\eta, \mathbf{k}) h_{ss}^{\lambda'(2)}(\eta, \mathbf{k}') \rangle + \langle h_{tt}^{\lambda(2)}(\eta, \mathbf{k}) h_{tt}^{\lambda'(2)}(\eta, \mathbf{k}') \rangle \\ &+ \langle h_{st}^{\lambda(2)}(\eta, \mathbf{k}) h_{st}^{\lambda'(2)}(\eta, \mathbf{k}') \rangle . \end{aligned} \quad (3.3)$$

Here we have used the fact that the two point function $\langle \zeta_{\mathbf{p}} h_{\mathbf{p}'} \rangle$ vanishes for any momenta \mathbf{p} , \mathbf{p}' . This can be seen as a consequence of the SVT theorem: everything decouples at linear order.

As stated in the introduction, the total power spectrum $\mathcal{P}_{h^{(2)}}$ can therefore be expressed as the sum of the three separate contributions \mathcal{P}_{ss} , \mathcal{P}_{tt} and \mathcal{P}_{st} , as

$$\langle h^{\lambda(2)}(\eta, \mathbf{k}) h^{\lambda'(2)}(\eta, \mathbf{k}') \rangle = \delta^{(3)}(\mathbf{k} + \mathbf{k}') \delta^{\lambda\lambda'} \frac{2\pi^2}{k^3} \{ \mathcal{P}_{ss} + \mathcal{P}_{tt} + \mathcal{P}_{st} \} . \quad (3.4)$$

It is useful to introduce the variables:

$$v = \frac{p}{k}, \quad u = \frac{|\mathbf{k} - \mathbf{p}|}{k} , \quad (3.5)$$

so that the integral over the wave-number $d^3\mathbf{p} = dp d\theta_p d\phi_p p^2 \sin\theta_p$ can be written as:

$$\int d^3\mathbf{p} = k^3 \int_0^\infty dv \int_{|v-1|}^{1+v} du (uv) \int_0^{2\pi} d\phi_p . \quad (3.6)$$

The reader can refer to App. D.1 to see how the functions presented in Eq. (2.16) are expressed in the new coordinate system.

In the following, we calculate each contribution to the power spectrum of SOGWs and assume no parity violation in the primordial tensor power spectrum.

3.1 Scalar-scalar power spectrum

In this section we present the results for the pure scalar contribution to the final power spectrum. This has also been done in Refs. [18, 40, 41], which the reader can refer to for more details. We need to consider: $\langle h_{ss}^{\lambda(2)}(\eta, \mathbf{k}) h_{ss}^{\lambda'(2)}(\eta, \mathbf{k}') \rangle$, which is given by:

$$\begin{aligned} \langle h_{ss}^{\lambda(2)}(\eta, \mathbf{k}) h_{ss}^{\lambda'(2)}(\eta, \mathbf{k}') \rangle &= \left(\frac{16}{9} \right)^2 \frac{1}{k^2 k'^2} \int \frac{d^3\mathbf{p}}{(2\pi)^{\frac{3}{2}}} \int \frac{d^3\mathbf{p}'}{(2\pi)^{\frac{3}{2}}} q^{\lambda,ss}(k, p) q^{\lambda',ss}(k', p') \\ &\times I^{ss}(x, v, u) I^{ss}(x', u', v') \langle \zeta_{\mathbf{p}} \zeta_{\mathbf{k}-\mathbf{p}} \zeta_{\mathbf{p}'} \zeta_{\mathbf{k}'-\mathbf{p}'} \rangle . \end{aligned} \quad (3.7)$$

The scalar four point function can be broken down into two-point correlations (Wick's theorem):

$$\begin{aligned} \langle \zeta_{\mathbf{p}} \zeta_{\mathbf{k}-\mathbf{p}} \zeta_{\mathbf{p}'} \zeta_{\mathbf{k}'-\mathbf{p}'} \rangle &= \langle \zeta_{\mathbf{p}} \zeta_{\mathbf{p}'} \rangle \langle \zeta_{\mathbf{k}-\mathbf{p}} \zeta_{\mathbf{k}'-\mathbf{p}'} \rangle + \langle \zeta_{\mathbf{p}} \zeta_{\mathbf{k}'-\mathbf{p}'} \rangle \langle \zeta_{\mathbf{k}-\mathbf{p}} \zeta_{\mathbf{p}'} \rangle \\ &= \delta(\mathbf{k} + \mathbf{k}') (\delta(\mathbf{p} + \mathbf{p}') + \delta(\mathbf{p} + \mathbf{k}' - \mathbf{p}')) \\ &\times \frac{2\pi^2}{p^3} \frac{2\pi^2}{|\mathbf{k} - \mathbf{p}|^3} \mathcal{P}_\zeta(p) \mathcal{P}_\zeta(|\mathbf{k} - \mathbf{p}|) . \end{aligned} \quad (3.8)$$

¹We do not include contributions from third order terms, such as $\langle h^\lambda(\eta, \mathbf{k}) h^{\lambda'(3)}(\eta, \mathbf{k}') \rangle$. We thank G. Domènech for pointing this out.

Inserting the above into Eq. (3.7) we find:

$$\begin{aligned} \langle h_{ss}^{\lambda(2)}(\eta, \mathbf{k}) h_{ss}^{\lambda'(2)}(\eta, \mathbf{k}') \rangle &= \delta^{(3)}(\mathbf{k} + \mathbf{k}') \delta^{\lambda\lambda'} \frac{2\pi^2}{k^3} \int_0^\infty du \int_{|1-u|}^{u+1} dv \frac{64}{81} \mathcal{P}_h(kv) \mathcal{P}_\zeta(ku) \\ &\times \frac{v^2}{u^2} \left(1 - \frac{(1v^2 - u^2)^2}{4v^2} \right)^2 \mathcal{I}_{ss}^2(x, v, u) \end{aligned} \quad (3.9)$$

and we can extract the power spectrum:

$$\mathcal{P}_{ss} = \frac{64}{81} \int_0^\infty dv \int_{|v-1|}^{1+v} du \frac{v^2}{u^2} \left(1 - \frac{(1v^2 - u^2)^2}{4v^2} \right)^2 \mathcal{I}_{ss}^2(x, v, u) \mathcal{P}_\zeta(ku) \mathcal{P}_\zeta(kv) \quad (3.10)$$

in agreement with the literature.

3.2 Tensor-tensor power spectrum

In this section we are interested in extracting the pure tensor power spectrum contribution, corresponding to $\langle h_{tt}^{\lambda(2)}(\eta, \mathbf{k}) h_{tt}^{\lambda'(2)}(\eta, \mathbf{k}') \rangle$ in Eq. (3.3):

$$\begin{aligned} \langle h_{tt}^{\lambda(2)}(\eta, \mathbf{k}) h_{tt}^{\lambda'(2)}(\eta, \mathbf{k}') \rangle &= \left(\frac{4}{\eta} \right)^2 \frac{1}{k^3 k'^3} \int \frac{d^3 \mathbf{p}}{(2\pi)^{\frac{3}{2}}} \int \frac{d^3 \mathbf{p}'}{(2\pi)^{\frac{3}{2}}} \left(q_1^{\lambda, tt}(k, p) \mathcal{I}_{tt,1}(x, v, u) \right. \\ &\quad \left. + q_2^{\lambda, tt}(k, p) \mathcal{I}_{tt,2}(x, v, u) \right) \left(q_1^{\lambda', tt}(k', p') \mathcal{I}_{tt,1}(x', u', v') \right. \\ &\quad \left. + q_2^{\lambda', tt}(k', p') \mathcal{I}_{tt,2}(x', u', v') \right) \langle h_{\mathbf{p}}^{\lambda_1} h_{\mathbf{k}-\mathbf{p}}^{\lambda_2} h_{\mathbf{p}'}^{\lambda'_1} h_{\mathbf{p}'-\mathbf{k}'}^{\lambda'_2} \rangle. \end{aligned} \quad (3.11)$$

The tensor four-point correlation function is given by:

$$\begin{aligned} \langle h_{\mathbf{p}}^{\lambda_1} h_{\mathbf{k}-\mathbf{p}}^{\lambda_2} h_{\mathbf{p}'}^{\lambda'_1} h_{\mathbf{p}'-\mathbf{k}'}^{\lambda'_2} \rangle &= \langle h_{\mathbf{p}}^{\lambda_1} h_{\mathbf{p}'}^{\lambda'_1} \rangle \langle h_{\mathbf{k}-\mathbf{p}}^{\lambda_2} h_{\mathbf{p}'-\mathbf{k}'}^{\lambda'_2} \rangle + \langle h_{\mathbf{p}}^{\lambda_1} h_{\mathbf{p}'-\mathbf{k}'}^{\lambda'_2} \rangle \langle h_{\mathbf{k}-\mathbf{p}}^{\lambda_2} h_{\mathbf{p}}^{\lambda'_1} \rangle \\ &= \delta(\mathbf{k} + \mathbf{k}') \left(\delta(\mathbf{p} + \mathbf{p}') \delta^{\lambda_1 \lambda'_1} \delta^{\lambda_2 \lambda'_2} + \delta(\mathbf{p} + \mathbf{k}' - \mathbf{p}') \delta^{\lambda_1 \lambda'_2} \delta^{\lambda_2 \lambda'_1} \right) \\ &\times \frac{2\pi^2}{p^3} \frac{2\pi^2}{|\mathbf{k} - \mathbf{p}|^3} \mathcal{P}_h(p) \mathcal{P}_h(|\mathbf{k} - \mathbf{p}|). \end{aligned} \quad (3.12)$$

Here $\delta^{\lambda_1 \lambda'_1}$ is the Kronecker delta which ensures the correct polarizations are selected. In App. C.1 we show that the integral over \mathbf{p} is invariant under $\mathbf{p} \rightarrow \mathbf{k} - \mathbf{p}$. This implies that when carrying out the integral over \mathbf{p}' the contribution from integrating over $\delta(\mathbf{p} + \mathbf{p}')$ or $\delta(\mathbf{p} + \mathbf{k}' - \mathbf{p}')$ is identical. By remembering that the Kronecker deltas multiplying these Dirac delta functions are ultimately switchable labels, we can carry out the integral over \mathbf{p}' in Eq. (3.11) over one of the Dirac deltas and multiply the final result by two. Switching to coordinates v and u and integrating over the azimuthal angle leads to:

$$\begin{aligned} \langle h_{tt}^{\lambda(2)}(\eta, \mathbf{k}) h_{tt}^{\lambda'(2)}(\eta, \mathbf{k}') \rangle &= \delta^{(3)}(\mathbf{k} + \mathbf{k}') \delta^{\lambda\lambda'} \frac{2\pi^2}{k^3} \int_0^\infty dv \int_{|v-1|}^{1+v} du \frac{1}{x^2} \mathcal{P}_h(ku) \mathcal{P}_h(kv) \\ &\left[\left(\frac{4v^2}{u^2} \left(1 - \frac{(1+v^2 - u^2)^2}{4v^2} \right)^2 \mathcal{I}_{tt,1}^2(x, v, u) \right) + \left(\frac{4}{k^4 u^2 v^2} \left(1 - \frac{(1+v^2 - u^2)^2}{4v^2} \right)^2 \mathcal{I}_{tt,2}^2(x, v, u) \right) \right. \\ &\quad \left. - \left(\frac{8}{k^2 u^2} \left(1 - \frac{(1+v^2 - u^2)^2}{4v^2} \right)^2 \mathcal{I}_{tt,1}(x, v, u) \mathcal{I}_{tt,2}(x, v, u) \right) \right], \end{aligned} \quad (3.13)$$

where the expressions that appear in front of the kernels result from integral of the polarization functions, as shown in App. C. Similarly to Ref. [40] we split our Kernels as:

$$\begin{aligned} \mathcal{I}_{tt,1}^2(x, v, u) &= \cos^2(x) [\mathcal{I}_{c,1}^{tt}(x, v, u)]^2 + \sin^2(x) [\mathcal{I}_{s,1}^{tt}(x, v, u)]^2 \\ &\quad + \sin(2x) \mathcal{I}_{c,1}^{tt}(x, v, u) \mathcal{I}_{s,1}^{tt}(x, v, u) , \end{aligned} \quad (3.14a)$$

$$\begin{aligned} \mathcal{I}_{tt,2}^2(x, v, u) &= \cos^2(x) [\mathcal{I}_{c,2}^{tt}(x, v, u)]^2 + \sin^2(x) [\mathcal{I}_{s,2}^{tt}(x, v, u)]^2 \\ &\quad + \sin(2x) \mathcal{I}_{c,2}^{tt}(x, v, u) \mathcal{I}_{s,2}^{tt}(x, v, u) , \end{aligned} \quad (3.14b)$$

$$\begin{aligned} \mathcal{I}_{tt,1}(x, v, u) \mathcal{I}_{tt,2}(x, v, u) &= \cos^2(x) \mathcal{I}_{c,1}^{tt}(x, v, u) \mathcal{I}_{c,2}^{tt}(x, v, u) + \sin^2(x) \mathcal{I}_{s,1}^{tt}(x, v, u) \mathcal{I}_{s,2}^{tt}(x, v, u) \\ &\quad + \cos x \sin x \mathcal{I}_{c,1}^{tt}(x, v, u) \mathcal{I}_{s,2}^{tt}(x, v, u) + \cos x \sin x \mathcal{I}_{s,1}^{tt}(x, v, u) \mathcal{I}_{c,2}^{tt}(x, v, u) \end{aligned} \quad (3.14c)$$

where

$$\mathcal{I}_{c,1}^{tt}(x, v, u) = \int_0^x d\bar{x} \sin(-\bar{x}) \bar{x} f_1^{tt}(\bar{x}, v, u) , \quad (3.15a)$$

$$\mathcal{I}_{s,1}^{tt}(x, v, u) = \int_0^x d\bar{x} \cos(\bar{x}) \bar{x} f_1^{tt}(\bar{x}, v, u) , \quad (3.15b)$$

$$\mathcal{I}_{c,2}^{tt}(x, v, u) = \int_0^x d\bar{x} \sin(-\bar{x}) \bar{x} f_2^{tt}(\bar{x}, v, u) , \quad (3.15c)$$

$$\mathcal{I}_{s,2}^{tt}(x, v, u) = \int_0^x d\bar{x} \cos(\bar{x}) \bar{x} f_2^{tt}(\bar{x}, v, u) . \quad (3.15d)$$

By comparing Eq. (3.4) to Eq. (3.13) it is straightforward to see what contributes to the final power spectrum:

$$\begin{aligned} \mathcal{P}_{tt} &= \frac{1}{x^2} \int_0^\infty dv \int_{|v-1|}^{1+v} du \left[1 - \frac{(1+v^2-u^2)^2}{4v^2} \right]^2 \mathcal{P}_h(ku) \mathcal{P}_h(kv) \\ &\quad \times \left(\frac{4v^2}{u^2} \mathcal{I}_{tt,1}^2(x, v, u) - \frac{8}{k^2 u^2} \mathcal{I}_{tt,1}(x, v, u) \mathcal{I}_{tt,2}(x, v, u) + \frac{4}{k^4 u^2 v^2} \mathcal{I}_{tt,2}^2(x, v, u) \right) . \end{aligned} \quad (3.16)$$

3.3 Scalar-tensor power spectrum

In this section we show how to extract the mixed-scalar power spectrum contribution, corresponding to $\langle h_{st}^{\lambda(2)}(\eta, \mathbf{k}) h_{st}^{\lambda'(2)}(\eta, \mathbf{k}') \rangle$ in Eq. (3.3):

$$\begin{aligned} \langle h_{st}^{\lambda(2)}(\eta, \mathbf{k}) h_{st}^{\lambda'(2)}(\eta, \mathbf{k}') \rangle &= \left(\frac{8}{3\eta} \right)^2 \frac{1}{k^3 k'^3} \int \frac{d^3 \mathbf{p}}{(2\pi)^{\frac{3}{2}}} \int \frac{d^3 \mathbf{p}'}{(2\pi)^{\frac{3}{2}}} q^{\lambda, st}(k, p) q^{\lambda', st}(k', p') \\ &\quad \times \mathcal{I}_{st}(x, v, u) \mathcal{I}_{st}(x', u', v') \langle h_{\mathbf{p}}^{\lambda_3} \zeta_{\mathbf{k}-\mathbf{p}} h_{\mathbf{p}'}^{\lambda'_3} \zeta_{\mathbf{k}'-\mathbf{p}'} \rangle . \end{aligned} \quad (3.17)$$

The four-point correlation function is given by:

$$\begin{aligned} \langle h_{\mathbf{p}}^{\lambda_3} \zeta_{\mathbf{k}-\mathbf{p}} h_{\mathbf{p}'}^{\lambda'_3} \zeta_{\mathbf{k}'-\mathbf{p}'} \rangle &= \langle h_{\mathbf{p}}^{\lambda_3} h_{\mathbf{p}'}^{\lambda'_3} \rangle \langle \zeta_{\mathbf{k}-\mathbf{p}} \zeta_{\mathbf{k}'-\mathbf{p}'} \rangle \\ &= \delta(\mathbf{k} + \mathbf{k}') \left(\delta(\mathbf{p} + \mathbf{p}') \delta^{\lambda_3 \lambda'_3} \right) \cdot \frac{2\pi^2}{p^3} \frac{2\pi^2}{|\mathbf{k} - \mathbf{p}|^3} \mathcal{P}_h(p) \mathcal{P}_\zeta(|\mathbf{k} - \mathbf{p}|) \end{aligned} \quad (3.18)$$

Following the same steps outlined in the previous section:

$$\begin{aligned} \langle h_{st}^{\lambda(2)}(\eta, \mathbf{k}) h_{st}^{\lambda'(2)}(\eta, \mathbf{k}') \rangle &= \delta^{(3)}(\mathbf{k} + \mathbf{k}') \delta^{\lambda \lambda'} \frac{2\pi^2}{k^3} \int_0^\infty du \int_{|1-u|}^{u+1} dv \frac{16}{9x^2} \mathcal{P}_h(kv) \mathcal{P}_\zeta(ku) \\ &\quad \times \frac{1}{k^4 u^2 v^2} M_{st}(v, u) \mathcal{I}_{st}^2(x, v, u) . \end{aligned} \quad (3.19)$$

The function $M_{st}(v, u)$ comes from the integration in the azimuthal direction and is defined in Eq. (C.14). Similarly, the kernels are split up as:

$$\begin{aligned} \mathcal{I}_{st}^2(x, v, u) &= \cos^2(x)[\mathcal{I}_c^{st}(x, v, u)]^2 + \sin^2(x)[\mathcal{I}_s^{st}(x, v, u)]^2 \\ &+ \sin(2x)\mathcal{I}_c^{st}(x, v, u)\mathcal{I}_s^{st}(x, v, u) , \end{aligned} \quad (3.20)$$

where

$$\mathcal{I}_c^{st}(x, v, u) = \int_0^x d\bar{x} \sin(-\bar{x})\bar{x} f^{st}(\bar{x}, v, u) , \quad (3.21a)$$

$$\mathcal{I}_s^{st}(x, v, u) = \int_0^x d\bar{x} \cos(\bar{x})\bar{x} f^{st}(\bar{x}, v, u) . \quad (3.21b)$$

Hence we have:

$$\mathcal{P}_{st} = \frac{1}{x^2} \frac{16}{9} \int_0^\infty dv \int_{|v-1|}^{1+v} du \mathcal{P}_h(kv) \mathcal{P}_\zeta(ku) M_{st}(v, u) \frac{1}{k^4 u^2 v^2} \mathcal{I}_{st}^2(x, v, u) . \quad (3.22)$$

4 Results: peaked power spectra

In this section we present our results: expressions for the current spectral density of SOGWs. Furthermore, we show the resulting spectral density for peaked power spectra sources, comment on the behaviour of the individual contributions as well as the total contribution. We also make some comments on detectability.

4.1 Current energy density of gravitational waves

The observable cosmologist use is the spectral density [49], related to the power spectrum by

$$\Omega_{GW}(\eta, k) = \frac{1}{6} \left(\frac{k}{\mathcal{H}(\eta)} \right)^2 \overline{\mathcal{P}_{h^{(2)}}(\eta, k)} , \quad (4.1)$$

where the overline here denotes an oscillation average over a few periods. Since these waves are generated in an early radiation dominated universe, we have to take into account how their density will change as the universe evolves. The density of gravitational waves scales like radiation and therefore it is possible to relate the spectral density at the time of creation, $\Omega_{GW}(k)$, to the present the spectral density, $\Omega_{GW}(\eta_0, k)$, which takes into account how the universe becomes matter dominated after the matter-radiation equality. For a detailed explanation the reader can refer to Ref. [18]:

$$\Omega_{GW}(\eta_0, k) h^2 = 1.62 \times 10^{-5} \times \Omega_{GW}(k) = 1.62 \times 10^{-5} \times \frac{1}{6} \frac{k^2}{\mathcal{H}(\eta)^2} \overline{\mathcal{P}_{h^{(2)}}(\eta, k)} , \quad (4.2)$$

where h is the dimensionless reduced Hubble constant to take into account the uncertainty in its value. Using $\mathcal{H}(\eta) = 1/\eta$ we define:

$$\Omega_{GW}(\eta_0, k) h^2 = 1.62 \times 10^{-5} \times \{ \Omega_{ss}(k) + \Omega_{tt}(k) + \Omega_{st}(k) \} , \quad (4.3)$$

where $\Omega_{ss}(k)$, $\Omega_{tt}(k)$ and $\Omega_{st}(k)$ are respectively the spectral density from the induced scalar-scalar, tensor-tensor and scalar-tensor at the time of creation. Below we present the corresponding expressions and their kernels which are the main results of our paper. To see

the details behind our kernel computations see App. D.2. We note that the spectral density depends on the time-averaged power spectrum. The time dependence in our expressions is contained in the kernels, via the variable $x = k\eta$, hence the following results are used to derive the final expressions:

$$\overline{\sin x} = \overline{\cos x} = 0, \quad \overline{\sin^2 x} = \overline{\cos^2 x} = \frac{1}{2}.$$

4.1.1 Spectral density of the scalar-scalar contribution

Inserting the power spectrum Eq. (3.10) into Eq. (4.1), we arrive to an expression for the spectral density from the scalar-scalar contribution

$$\Omega_{ss}(k) = \frac{32}{243} \int_0^\infty dv \int_{|v-1|}^{1+v} du \left(\frac{4v^2 - (1 + v^2 - u^2)^2}{4uv} \right)^2 \overline{\mathcal{I}_{ss}^2(v, u)} \mathcal{P}_\zeta(ku) \mathcal{P}_\zeta(kv), \quad (4.4)$$

with

$$\begin{aligned} \overline{\mathcal{I}_{ss}^2(v, u)} = & 2^2 \frac{1}{2} \left(\frac{3(u^2 + v^2 - 3)}{4u^3v^3} \right)^2 \left[\left(-4uv + (u^2 + v^2 - 3) \log \left| \frac{3 - (u+v)^2}{3 - (u-v)^2} \right| \right)^2 \right. \\ & \left. + \pi^2 (u^2 + v^2 - 3)^2 \Theta(v + u - \sqrt{3}) \right]. \end{aligned} \quad (4.5)$$

The expression for the Kernel has been taking from Ref. [41]. The factor of 2^2 in front comes from the difference in decomposing the metric in our two papers.

4.1.2 Spectral density of the tensor-tensor contribution

Similarly, the tensor-tensor spectral density is given by:

$$\begin{aligned} \Omega_{tt}(k) = & \frac{1}{6} \int_0^\infty dv \int_{|v-1|}^{1+v} du \left[1 - \frac{(1 + v^2 - u^2)^2}{4v^2} \right]^2 \mathcal{P}_h(ku) \mathcal{P}_h(kv) \\ & \times \left(\frac{4v^2}{u^2} \overline{\mathcal{I}_{tt,1}^2(v, u)} - \frac{8}{k^2 u^2} \overline{\mathcal{I}_{tt,1}(v, u) \mathcal{I}_{tt,2}(v, u)} + \frac{4}{k^4 u^2 v^2} \overline{\mathcal{I}_{tt,2}^2(v, u)} \right), \end{aligned} \quad (4.6)$$

The time-averaged kernels are shown below:

$$\overline{\mathcal{I}_{tt,1}^2(v, u)} = \frac{1}{32u^2v^2} \left(\pi^2 \Theta(u + v - 1) + \log \left| \frac{1 - (u+v)^2}{1 - (u-v)^2} \right|^2 \right), \quad (4.7a)$$

$$\overline{\mathcal{I}_{tt,2}^2(v, u)} = \frac{k^4}{128u^2v^2} \left(\pi^2 (u^2 + v^2 - 1)^2 \Theta(u + v - 1) + \left(\log \left| \frac{1 - (u+v)^2}{1 - (u-v)^2} \right| - 4vu \right)^2 \right), \quad (4.7b)$$

$$\begin{aligned} \overline{\mathcal{I}_{tt,1}(v, u) \mathcal{I}_{tt,2}(v, u)} = & \frac{k^2}{64u^2v^2} \left(\pi^2 (u^2 + v^2 - 1) \Theta(u + v - 1) + \log \left| \frac{1 - (u+v)^2}{1 - (u-v)^2} \right| \left(-4vu \right. \right. \\ & \left. \left. + \log \left| \frac{1 - (u+v)^2}{1 - (u-v)^2} \right| \right) \right). \end{aligned} \quad (4.7c)$$

4.1.3 Spectral density of the scalar-tensor contribution

Finally, the spectral density of scalar-tensor induced gravitational waves reads:

$$\Omega_{st}(k) = \frac{32}{243} \int_0^\infty dv \int_{|v-1|}^{1+v} du \mathcal{P}_h(kv) \mathcal{P}_\zeta(ku) \frac{1}{k^4 u^2 v^2} M_{st}(v, u) \overline{\mathcal{I}_{st}^2(v, u)}, \quad (4.8)$$

with:

$$\begin{aligned} \overline{\mathcal{I}_{st}^2(v, u)} = & \frac{9k^4}{2048v^2u^6c_s^6} \left(\pi^2 (i_-^{st}(v, u))^2 \Theta(v + uc_s - 1) + \left(i_+^{st}(v, u) \log \left| \frac{c_s u - v - 1}{c_s u + v + 1} \right| \right. \right. \\ & \times (c_s u - v - 1)(c_s u + v + 1) + i_-^{st}(v, u) \log \left| \frac{c_s u - v + 1}{c_s u + v - 1} \right| (c_s u - v + 1)(c_s u + v - 1) \\ & \left. \left. - 20c_s uv \left[-\frac{3}{5} + \frac{v^2}{5}(7 - c_s^2) + \frac{8uv}{5} + u^2 \left(c_s^4 - \frac{7c_s^2}{15} + \frac{4}{5} \right) - \frac{9c_s^2}{5} \right] \right)^2 \right). \quad (4.9) \end{aligned}$$

The function $i_\pm^{st}(v, u)$ is defined as:

$$i_\pm^{st}(v, u) = -1 + 4u^2 - 3c_s^2(u^2 + (v \pm 1)^2 - c_s^2 u^2) + 8uv + v(\mp 2 + 7v). \quad (4.10)$$

4.2 Comments on potential divergences and resonances

The behaviour of the integrands (4.4), (4.6) and (4.8) in the IR and UV limits contains information of any possible divergences that may appear. The IR limit (long wave-length) corresponds to taking $k \rightarrow 0$, then $v \rightarrow 1/k$ and $u \rightarrow 1/k$, and all three contributions are well behaved in this limit. In fact, in the IR limit the scalar-scalar induced waves have a log-dependent slope [34] and it was shown that this is not the case for the scalar-tensor induced waves due to scalar and tensor fluctuations not having the same propagation speed [37].

In the UV limit (short wave-length), as $k \rightarrow \infty$, we have $v \rightarrow 0$ and $u \rightarrow 1$ for the pure quadratic contributions. The scalar-scalar limit is finite, whilst the tensor-tensor limit goes as v^{-2} . For the cross scalar-tensor term, taking the UV limit breaks the symmetry we have between v and u , there are now two distinct limits: $v \rightarrow 0$ and $u \rightarrow 1$, corresponding to the large wavelength for tensors, and $v \rightarrow 1$ and $u \rightarrow 0$ corresponding to the large wavelength for scalars. In the former case the integrand diverges as v^{-4} whilst in the latter as u^{-6} . Hence we see that if the first order power spectra are given by a power law, below a certain order, there could be an unphysical contribution to the final spectral density. This was first pointed out for the scalar-tensor case in Ref. [37].

Furthermore, the scalar-scalar, tensor-tensor and scalar-tensor integrands contain logarithmic terms that could lead to possible divergences, provided v and u take particular values. By considering ‘momentum conservation’ we can extract a range allowed values for v and u . The wave vectors in Fourier space of the three modes form a triangle, with sides: \mathbf{k} , \mathbf{p} and $\mathbf{k} - \mathbf{p}$, where the magnitude of the vectors satisfy the triangle inequality, which in terms of the variables v and u is given by: $|u - v| < 1 < u + v$. Hence, we see that the tensor-tensor spectral density will not enter a logarithmic resonance since the value of v and u needed do not satisfy the triangle inequality. On the other hand, the scalar-scalar contribution can enter into a logarithmic resonance when $v + u = \sqrt{3}$ since this corresponds to a possible configuration of the wave-vectors. Similarly, there is a possible logarithmic divergence for the scalar-tensor contribution when $v = 1 \pm c_s u$, but this is prevented from the terms multiplying the logarithmic terms. However, in the limit $v \rightarrow 1 \pm c_s u$ the scalar-tensor integrand tends to u^{-6} which causes a divergences in the large scalar wavelength limit.

For the reasons outlined above we will exclusively input peaked power spectra, which we do in the following sections, by first looking at the result induced waves from a monochromatic power spectra and secondly lognormal power spectra.

4.3 Monochromatic power spectra

It is informative to study the spectrum of SOGWs that results from having a sharp peak in the input power spectrum, modelled by a Dirac delta function. Although ‘not physical’ (i.e. there is no such thing as a infinitely sharp peak in nature), the resulting spectral density tells us a lot about the properties and shape of resulting spectra in general.

The monochromatic power spectrum is given by

$$\mathcal{P}_{\zeta,h}(k) = \mathcal{A}_{\zeta,h} \delta\left(\log \frac{k}{k_{\zeta,h}}\right), \quad (4.11)$$

with $\mathcal{A}_{\zeta,h}$ the amplitude of the power spectrum and $k_{\zeta,h}$ the location of the scalar and tensor peak in the primordial power spectrum, respectively. Hence we get

$$\mathcal{P}_{\zeta,h}(kv) = \mathcal{A}_{\zeta,h} \delta\left(\log \frac{kv}{k_{\zeta,h}}\right) = \mathcal{A}_{\zeta,h} \frac{k_{\zeta,h}}{k} \delta\left(v - \frac{k_{\zeta,h}}{k}\right). \quad (4.12)$$

The same holds for $\mathcal{P}_{\zeta,h}(ku)$, if we swap $v \leftrightarrow u$. The way we have expressed the power spectrum makes it straightforward to use the sifting property of the Dirac delta function, we just have to take the limits of integration of Eqs. (4.4), (4.6) and (4.8) into account

$$\begin{cases} |1-v| < u < 1+v \\ 0 < v < \infty \end{cases} = \begin{cases} |k-k_h| < k_\zeta < k+k_h \\ 0 < k_h/k < \infty \end{cases} = |k_\zeta - k_h| < k < k_\zeta + k_h. \quad (4.13)$$

Below we study two different scenarios: first, the case where the primordial power spectrum for scalars and tensors peaks at the same scale and then the case where the two peaks are at different scales.

4.3.1 Peak at the same scale

In this section, the primordial power spectrum of scalar and tensor perturbations peaks at the same scale so that $k_\zeta = k_h \equiv k_p$. The inequality (4.13) reduces to: $0 < k < 2k_p$, which can be encoded by a Heaviside step function. For convenience, we define $\tilde{k} = k/k_p$.

The analytic expression for scalar-scalar part Eq. (4.4) is

$$\Omega_{ss}(k) = \frac{32}{243} \mathcal{A}_\zeta^2 \tilde{k}^{-2} \left(\frac{\tilde{k}^2 - 4}{4}\right)^2 \overline{\mathcal{I}^{ss}(v = \tilde{k}^{-1}, u = \tilde{k}^{-1})^2} \Theta(2k_p - k). \quad (4.14)$$

The resulting behaviour of Eq. (4.14) is shown in Fig. 1. There is a sharp peak at $\tilde{k} = 2/\sqrt{3}$, or when $k = 2c_s k_p$, which corresponds to $u + v = \sqrt{3}$ as expected following our discussion on resonances in the scalar-scalar SOGWs in Sect. 4.2. Furthermore, due to momentum conservation, there is the expected sharp cutoff at $k = 2k_p$.

For the Dirac peaked spectra the tensor-tensor part Eq. (4.6)

$$\begin{aligned} \Omega_{tt}(k) = & \frac{2}{3} \mathcal{A}_h^2 \left(\frac{\tilde{k}^2 - 4}{4}\right)^2 \left(\frac{4}{\tilde{k}^2} \overline{\mathcal{I}_{tt,1}(v = \tilde{k}^{-1}, u = \tilde{k}^{-1})^2} + \frac{4\tilde{k}^2}{k^4} \overline{\mathcal{I}_{tt,2}(v = \tilde{k}^{-1}, u = \tilde{k}^{-1})^2} \right. \\ & \left. - \frac{8}{\tilde{k}^2} \overline{\mathcal{I}_{tt,1}(v = \tilde{k}^{-1}, u = \tilde{k}^{-1})} \times \overline{\mathcal{I}_{tt,2}(v = \tilde{k}^{-1}, u = \tilde{k}^{-1})} \right) \Theta(2k_p - k). \end{aligned} \quad (4.15)$$

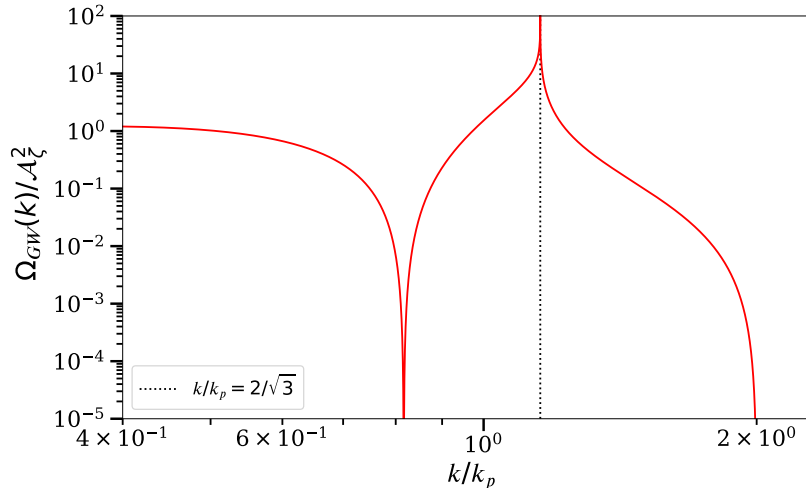


Figure 1: The spectral density $\Omega_{ss}(k)$ of second order gravitational waves induced by scalar-scalar modes, normalised by \mathcal{A}_ζ , against a range of k around some pivot scale k_p . There is a logarithmic resonance that occurs when $\tilde{k} = 2/\sqrt{3}$, represented by the black-dotted line, as expected from looking at the kernel (4.5). After the peak, the spectral density decreases rapidly before hitting the cut-off at $k = 2k_p$.

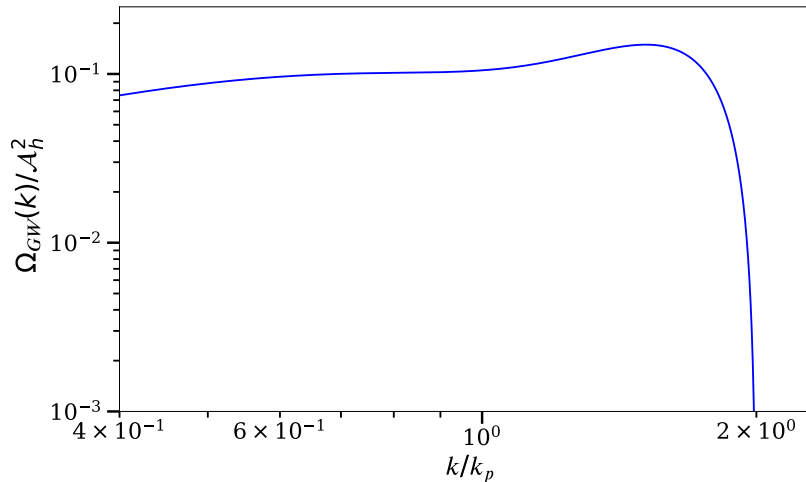


Figure 2: The spectral density $\Omega_{tt}(k)$ of second order gravitational waves induced by tensor-tensor modes, normalised by \mathcal{A}_h , against a range of k around some pivot scale k_p . There is no logarithmic resonance since the magnitude of the wave-vectors needed for the resonance, $u + v = 1$, are not allowed due to momentum conservation. The orders of magnitude spanned by the tensor-tensor contribution peaks just above 10^{-1} , an amplitude much smaller than the scalar-scalar induced waves.

Equation (4.15) is plotted in Fig 2. We note that, as expected, for tensor-tensor induced gravitational waves there is no resonant peak.

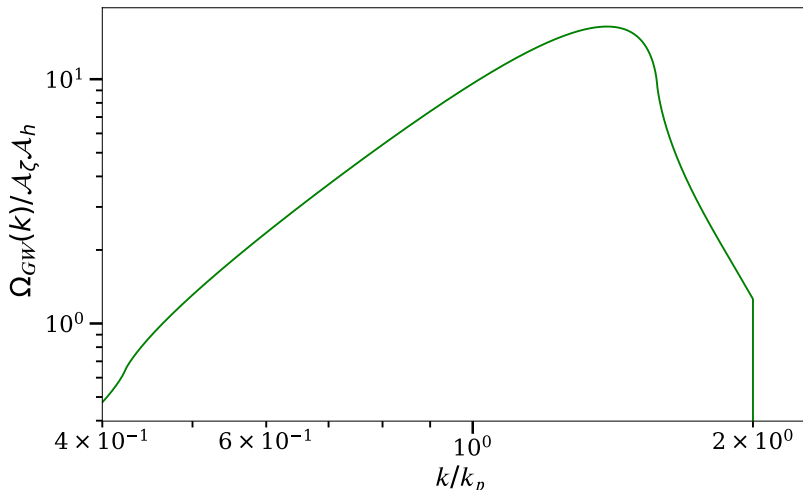


Figure 3: The spectral density of second order gravitational waves induced by scalar-tensor modes, where the primordial power spectra peak at the same scale k_p . The values needed to have a logarithmic resonance are allowed by momentum conservation but due to the structure of (4.9), the resonance does not occur. The amplitude spanned by the scalar-tensor induced waves is comparable to the scalar-scalar case.

The scalar-tensor or cross-term part of Eq. (4.8) is given by

$$\Omega_{st}(k) = \frac{8}{27} \mathcal{A}_\zeta \mathcal{A}_h \frac{\tilde{k}^2}{k^4} M_{st}(v = \tilde{k}^{-1}, u = \tilde{k}^{-1}) \overline{\mathcal{I}_{st}(k, v = \tilde{k}^{-1}, u = \tilde{k}^{-1})^2} \Theta(2k_p - k). \quad (4.16)$$

Equation (4.16) is shown in Fig. 3. As expected, there is no resonant behavior. Furthermore, we have compared our results with the results in Ref. [37]² and find that our spectral densities have an overall similar behaviour.

Finally, we can compare all three contributions to the total spectral density, shown in Fig. 4. We see that the tensor-tensor contribution is several orders of magnitude smaller than the other two types of sources. This is partly due to the fact that the amplitude of the primordial tensor power spectrum is smaller than the primordial scalar power spectrum but this is not solely the reason. Expanding the expressions for the spectral density in k for the scalar-scalar contribution (4.14) and the scalar-tensor contribution (4.16), we see that the highest power of k is k^{14} whilst for the tensor-tensor contribution (4.15) it is k^{10} . This implies that the nature of the tensor-tensor source terms inherently makes them a smaller contribution as compared to the other modes of production. The second aspect of Fig. 4 that is important is the behaviour of the total spectral density for high values of k . The scalar-scalar contribution drops around four orders of magnitude between the resonant peak and the cut-off at $k = 2k_p$, whilst the scalar-tensor contribution does not drop off and stays roughly constant until the cut-off. This shows that the mixed contribution is in fact important and must be taken into account, if there is a peak in the primordial scalar and tensor power spectrum.

We find that the total induced gravitational wave spectrum is in overall agreement with the results in Ref. [20] (see the blue curve in their Fig. 2). However we found that the

²See their Eqs. (3.12) and (4.2) for comparison.

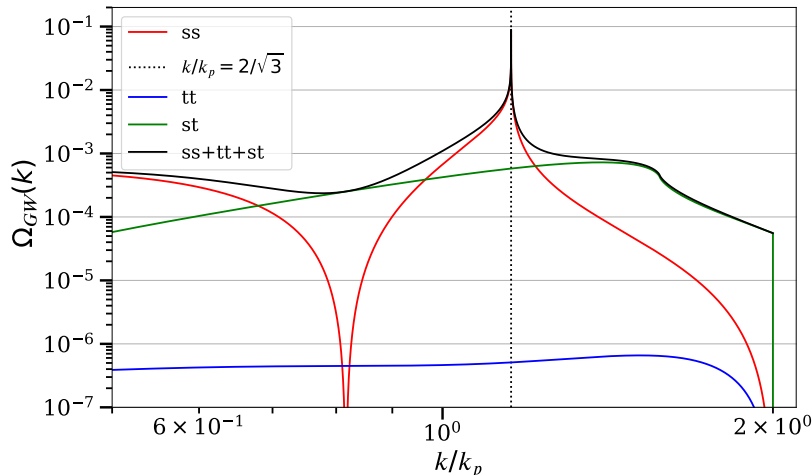


Figure 4: The total spectral density, where we have set $\mathcal{A}_h = 0.1\mathcal{A}_\zeta$. The tensor-tensor contribution (blue line) is subdominant compared to the scalar-scalar (red line) and scalar-tensor (green line) contributions. This is not only due to the fact that the amplitude of the primordial power spectrum for tensors is smaller than the one for scalars, but mainly due to the structure of the tensor-tensor source terms. Secondly, when considering the total contribution to the induced waves (black line) it becomes clear that for high values of k the scalar-tensor contribution becomes the dominant mode of production for induced gravitational waves in this case.

amplitude of the spectral density drops off more steeply after the resonant peak on small scales.

4.3.2 Peaks at a different scale

In this section we show how the second order scalar-tensor power spectrum changes when the primordial power spectra for scalars and tensors peak at different scales. The expression for the spectral density becomes

$$\begin{aligned} \Omega_{st}(k) = & \frac{2}{27} \mathcal{A}_\zeta \mathcal{A}_h \frac{1}{k^2 k_\zeta k_h} M_{st}(v = k_h/k, u = k_\zeta/k) \overline{\mathcal{I}_{st}(k, v = k_h/k, u = k_\zeta/k)^2} \\ & \times \Theta(k - |k_\zeta - k_h|) \Theta(-k + k_\zeta + k_h), \end{aligned} \quad (4.17)$$

where the two Heaviside step functions encode the integral limits in Eq. (4.13). We look at two different informative cases: first when the tensor power spectrum peaks at a scale higher than the resonance from the scalar-scalar contribution ($k_h \approx c_s k_\zeta$), and then at a scale smaller than the resonance ($k_h \approx 4c_s k_\zeta$). The results are presented in Fig. 5. We see that when $k_h \approx c_s k_\zeta$ the scalar-tensor contribution is smaller than when the power spectra peak at the same scale, in fact we chose this value for k_h because this value corresponds to an approximate threshold: when $k_h \leq c_s k_\zeta$ the signal will always be smaller than the case when $k_h = k_\zeta$. Secondly, we chose the peak scale $k_h \approx 4c_s k_\zeta$ to show that we can get higher amplitude signals than the previous setup. The short ‘burst’ like signal is due to the allowed k values encoded in the Heaviside step functions in Eq. (4.17). Indeed, the closer k_h is k_ζ the more the range of k increases. In Fig. 6 we show all three contributions to the spectral density. The sharp feature in this signal is due to the fact that the input is a Dirac delta power spectrum.

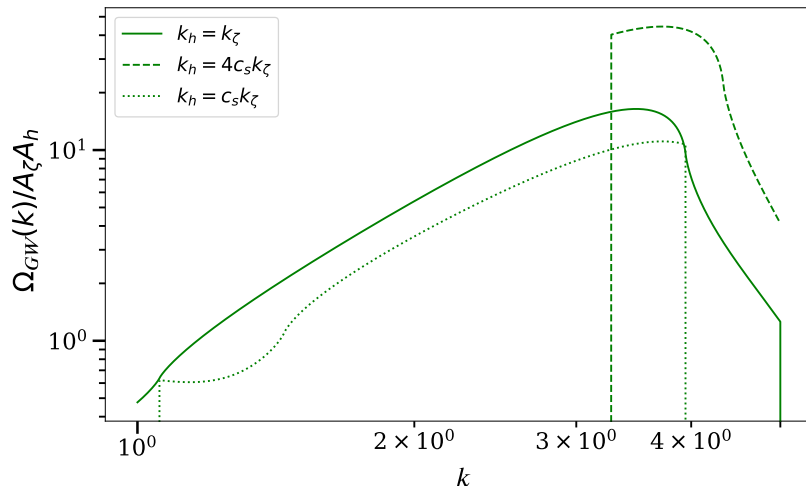


Figure 5: The spectral density of gravitational waves induced by scalar-tensor modes for a range of k values. Here we present three different scenarios: when the primordial power spectra peak at the same scale (solid line), when the primordial tensor peaks on larger scales than the scalar-scalar resonant peak (dotted line), and when the primordial tensor peaks on smaller scales than the scalar-scalar resonant peak (dashed line). The ‘impulse’ like behaviour of the dashed line can be understood from momentum conservation encoded in the Heaviside step functions.

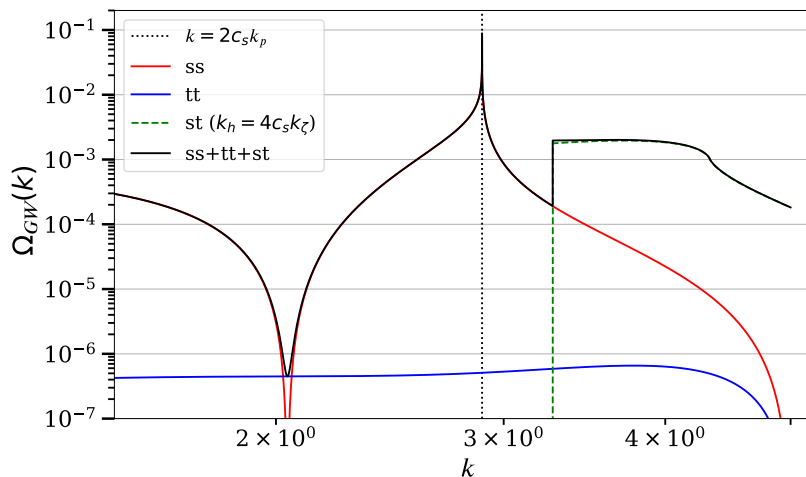


Figure 6: Full spectral density, where we have set $\mathcal{A}_h = 0.1\mathcal{A}_\zeta$, with the scalar-tensor contribution (dashed green line) this time coming from a primordial power spectrum which peaks at a smaller scale than the scalar-scalar resonance.

4.4 Lognormal Peak

As discussed earlier, a Dirac delta peak is not realistic, and hence to discuss the plausibility of detecting these induced waves we should move to a power spectrum which has some finite

width to its peak. This can be achieved with a Lognormal power spectrum,

$$\mathcal{P}_{\zeta,h} = \frac{\mathcal{A}_{\zeta,h}}{\sqrt{2\pi}\sigma} \exp\left(-\frac{\log^2(k/k_{\zeta,h})}{2\sigma^2}\right), \quad (4.18)$$

with σ controlling the width of the peak and normalised such that $\int_{-\infty}^{\infty} d\log k \mathcal{P}_{\zeta,h} = \mathcal{A}_{\zeta,h}$. In the following we take $\sigma = 0.1$, so that the general behaviour of the spectral densities discussed in the previous section (Dirac delta input power spectra), holds in this scenario. For a detailed discussion of scalar-scalar induced waves from a lognormal peak, see Ref. [44]. The scale at which we centre the scalar power spectrum (k_{ζ}) is chosen so that the physical frequency is centred in the LISA band: $k = f \times (2\pi a_0)$, with $f_{\zeta} = 3.4$ mHz. We take $\mathcal{A}_{\zeta} \approx 2.1 \times 10^{-2}$, which corresponds to an enhancement of $\mathcal{O}(10^7)$ of the Planck 2018 data [47], motivated by the enhancement needed to the power spectrum in order to produce primordial black holes [24]. All spectral densities in the following are found by numerically integrating the expressions in Eqs. (4.4), (4.6) and (4.8). In Fig. 7 we present the results of our toy model for different scenarios. We consider the cases where the power spectrum of scalars and tensors peak at identical and different scales for different values of \mathcal{A}_h relative to \mathcal{A}_{ζ} . A feature that becomes apparent is that when $\mathcal{A}_h = \mathcal{A}_{\zeta}$ and $k_h = k_{\zeta}$ (top-left plot in Fig. 7), the scalar-tensor contribution becomes dominant. This could be due to the fact that the scalar-scalar resonance is less sharp and hence has lower amplitude than in the Dirac delta case. When we decrease the amplitude of the tensor power spectrum by a factor of ten (bottom-left plot in Fig. 7) the resonant behaviour becomes apparent in the total signal and the scalar-tensor signal contributes narrowly on smaller scales. For the case when $k_h = 4c_s k_{\zeta}$ (top and bottom right plots in Fig. 7) we can still distinguish the resonant peak and also have an extra contribution coming from the scalar-tensor terms, in the form of a peak.

5 Discussion

In higher order cosmological perturbation theory lower order terms can couple to source the higher order terms. Hence second order gravitational waves will be sourced by coupled first order scalar, vector, and tensor terms. Until recently, research has focused on source terms which are quadratic in first order scalar fluctuations, so-called SIGWs (see e.g. Ref. [18]). In this paper, we investigated what happens if we include first order tensor fluctuations to contribute as a possible source. Two new sources appear: terms quadratic in tensor fluctuations and terms that couple a scalar and a tensor fluctuation. We have shown that the tensor-tensor contribution is subdominant due to its inherit structure whilst the scalar-tensor contribution is non negligible, particularly on small scales, in agreement with recent studies [20, 37, 38]. Analytical results for the spectral density and kernels for the scalar-scalar, tensor-tensor and scalar-tensor contribution can be found in Sec. 4.1.1, 4.1.2 and Sec. 4.1.3 respectively.

In a Λ CDM universe, SOGWs sourced during the radiation dominated epoch of universe have a distinctive signal compared to the SIGWs. Due to the behaviour of source terms including tensors in the UV limit, we studied the spectral density of waves induced by peaked spectra. Particularly, we showed if there is peak in the first order tensor power spectrum, then the overall spectral density will be different to waves induced by quadratic scalar fluctuations. First of all, in the case of the primordial power spectra having the same amplitude, the scalar-tensor contribution becomes dominant in the power spectrum and if the primordial spectra peak at the same scale the distinctive resonant behaviour of SIGWs is not apparent anymore.

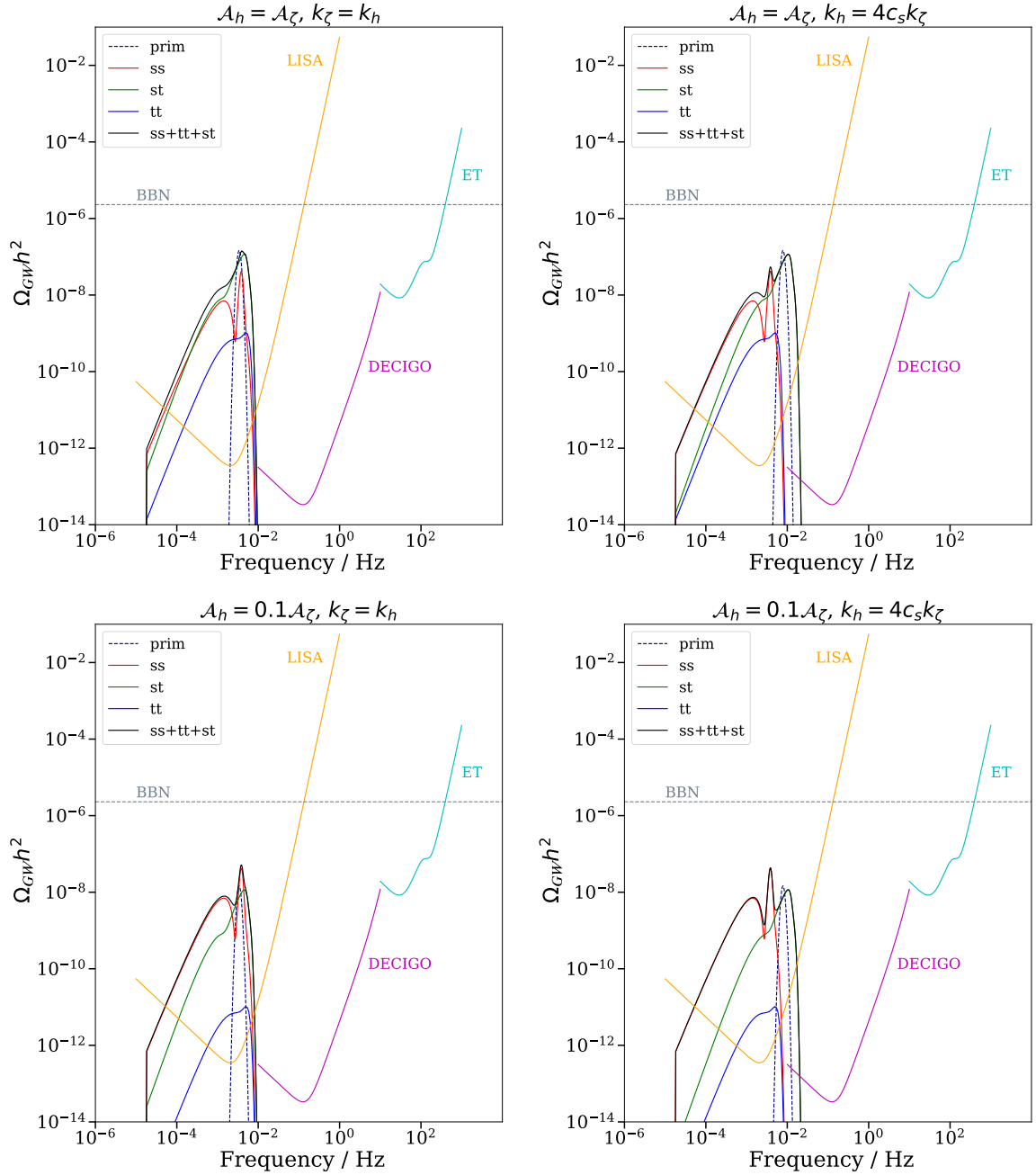


Figure 7: Plots of the spectral density against frequency. Each graph corresponds to a different setup in the value of \mathcal{A}_ζ , \mathcal{A}_h , k_ζ and k_h . We have also included the noise power spectral densities curves [35] for LISA, ET [45] and DECIGO [32], as well as bounds on primordial gravitational waves from BBN [46]. Furthermore, the dashed dark blue line is the primordial tensor power spectrum. We see that the scalar-tensor contribution is non-negligible and in some cases dominant. The sharp signals on larger scales and below the threshold for detection are artifacts of numerical integration.

We also showed that when the primordial tensor power spectrum peaks at smaller scale then

the scalar one, the spectral density gets an additional contribution which shows up as an additional peak (see Fig. 7). Since the power spectrum for first order scalars and tensors is directly linked to inflation, our results can be used to constrain certain models which have a peak in the primordial tensor power spectrum.

Work on second order gravitational waves, sourced by first order scalar and tensor modes has so far focused mainly on toy model input power spectra. A natural next step is therefore to use more realistic input power spectra, both for the scalar and the tensor perturbations. In most cases this will no longer allow the use of analytical techniques and will require the use of numerical methods. Luckily there are already numerical packages to calculate the power spectrum for any single or multi-field model available, such as PyTransport [50]. In a future extension of the work presented here we therefore plan to combine our results with PyTransport, which will allow us to further constrain the parameter space of models of inflation using gravitational waves.

Acknowledgments

The authors thank Chris Addis, Pedro Carrilho, Chris Clarkson, Charles Dalang, Matthew Davies, Pedro Fernandes, Laura Iacconi and David Mulryne for useful discussions. The authors are also grateful to Guillem Domènech for useful discussions and sharing an early draft of their work. RP is funded by STFC grant ST/P000592/1 and KAM is supported in part by STFC grant ST/T000341/1.

Note added. Whilst in the final stages of this project, Ref. [37] and Ref. [38] were published on the arXiv.

A Evolution equations

Below we give the background, first order and second order relevant Einstein equations. We have used the *xPand* package [48] for our computations. All calculations carried out below are done in the Newtonian gauge.

A.1 Background equations

The energy-momentum tensor is given in Eq. (2.4). At 0th order (background), the two Friedmann equations are

$$\mathcal{H}^2 = \frac{a^2}{3M_{Pl}^2}\rho, \quad \mathcal{H}' = -\frac{a^2\rho}{6M_{Pl}^2}(1+3w), \quad \text{with } P = w\rho, \quad (\text{A.1})$$

where w is the equation of state parameter. There is also a conservation equation

$$\rho' + 3\mathcal{H}(\rho + P) = 0. \quad (\text{A.2})$$

From the above we infer that during RD ($w = 1/3$):

$$a(\eta) \propto \eta, \quad \mathcal{H} = \frac{1}{\eta}. \quad (\text{A.3})$$

A.2 First order equations

The source terms in Eq. (2.7) have been simplified using first order relations we obtain from the Einstein equations, below we present only the relevant ones. The first order density perturbation and the scalar part of the velocity perturbation can be related to metric variables, from the 0 – 0 and by taking the divergence of the 0 – i first order Einstein equations respectively, we arrive to

$$\delta\rho = -2\rho\Phi + \frac{M_{Pl}^2}{a^2}(-6\mathcal{H}\Psi' + 2\nabla^2\Psi), \quad (\text{A.4})$$

$$v = -\frac{2}{3(1+w)\mathcal{H}}\left(\Phi + \frac{\Psi'}{\mathcal{H}}\right). \quad (\text{A.5})$$

Furthermore, in the case of vanishing anisotropic stress, the symmetric trace-free part of the Einstein equations for a perfect fluid implies $\Phi = \Psi$. This simplifies the calculations significantly, namely we can get an evolution equation for Ψ (the trace of the spatial part of the Einstein equations) in Fourier space:

$$\Psi'' + 3\mathcal{H}(1 + c_s^2)\Psi' + c_s^2k^2\Psi = 0. \quad (\text{A.6})$$

The solution to this equation is shown in Eq. (2.12). We have introduced the speed of sound:

$$\delta P = c_s^2\delta\rho, \quad (\text{A.7})$$

for adiabatic perturbations. We further note that when the equation of state is constant, then $c_s^2 = w$, as is the case in our work.

Additionally, we are interested in the first order tensor evolution equation, using the TT projector, defined in Eq. (2.2), on the first order spatial Einstein equations we arrive at

$$h''_{ij} + 2\mathcal{H}h'_{ij} - \nabla^2 h_{ij} = 0. \quad (\text{A.8})$$

The solution to the first order tensor mode equation is shown in Eq. (2.13).

A.3 Second order equations

The spatial part of the second order Einstein tensor is given by:

$$\begin{aligned}
G_{ij}^{(2)} = & h_{ij}''^{(2)} + 2\mathcal{H}h_{ij}'^{(2)} - h_{ij}^{(2)}(2\mathcal{H}^2 + 4\mathcal{H}') - \nabla^2 h_{ij}^{(2)} + \delta_{ij}(\Phi^{(2)} + \Psi^{(2)})(2\mathcal{H}^2 + 4\mathcal{H}') \\
& + 2\delta_{ij}\Phi'^{(2)}\mathcal{H} + 4\delta_{ij}\Psi'^{(2)}\mathcal{H} + 2\delta_{ij}\Psi''^{(2)} + \delta_{ij}\nabla^2\Phi^{(2)} - \delta_{ij}\nabla^2\Psi^{(2)} \\
& - \partial_i\partial_j\Phi^{(2)} + \partial_i\partial_j\Psi^{(2)} - 4h_i^{m'}h_{jm}' + \delta_{ij}\left(3h_{mk}'h^{mk'} + 4h^{mk}h_{mk}'' + 8\mathcal{H}h^{mk}h_{mk}'\right) \\
& - \Phi\left(4h_{ij}'' + 8\mathcal{H}h_{ij}' - 8\mathcal{H}^2h_{ij} - 16\mathcal{H}'h_{ij}\right) - \delta_{ij}\left(8\mathcal{H}^2 + 16\mathcal{H}'\right)\Phi^{(2)} - 16\delta_{ij}\mathcal{H}\Phi\Phi' \\
& + \Phi'\left(8\mathcal{H}h_{ij} - 2h_{ij}'\right) + \delta_{ij}\left(16\mathcal{H}' - 8\mathcal{H}^2\right)\Phi\Psi - 8\delta_{ij}\mathcal{H}\Psi\Phi' + 2h_{ij}'\Psi' + 24\mathcal{H}h_{ij}\Psi' \\
& - 16\delta_{ij}\mathcal{H}\Phi\Psi' - 4\delta_{ij}\Phi'\Psi' + 2\delta_{ij}\Psi'^2 + 12h_{ij}\Psi'' - 8\delta_{ij}\Phi\Psi'' - 4\Psi\nabla^2h_{ij} + 4h_i^m\partial_m\partial_j\Psi, \\
& + (4h_{ij} - 4\delta_{ij}\Phi)\nabla^2\Phi - (8h_{ij} + 4\delta_{ij}\Psi)\nabla^2\Psi + 4h_j^m\partial_m\partial_i\Psi - 2\partial_k h_{ij}\partial^k\Phi \\
& - 2\delta_{ij}\partial_k\Phi\partial^k\Phi - 6\partial_k h_{ij}\partial^k\Psi - 4\delta_{ij}\partial_k\Psi\partial^k\Psi + 4h^{mk}\partial_m\partial_k h_{ij} - 4h^{mk}\delta_{ij}\partial_m\partial_k\Phi \\
& - 4\partial_m h_{jk}\partial^k h_i^m + 4\partial_k h_{jm}\partial^k h_i^m - 4h^{mk}\delta_{ij}\nabla^2 h_{mk} + 2\delta_{ij}\partial_k h_{md}\partial^d h^{mk} \\
& - 3\delta_{ij}\partial_d h_{mk}\partial^d h^{mk} + 2\partial^m\Phi\partial_i h_{jm} + 2\partial^m\Psi\partial_i h_{jm} - 4h^{mk}\partial_i\partial_k h_{jm} + 2\partial_i h^{mk}\partial_j h_{mk} \\
& + 2\partial^m\Psi\partial_j h_{im} + 2\partial^m\Phi\partial_j h_{im} + 2\partial_i\Phi\partial_j\Phi - 2\partial_i\Psi\partial_j\Phi - 2\partial_i\Phi\partial_j\Psi + 6\partial_i\Psi\partial_j\Psi \\
& - 4h^{mk}\partial_j\partial_k h_{im} + 4h^{mk}\partial_j\partial_i h_{mk} + 4\Phi\partial_j\partial_i\Phi + 4\Psi\partial_j\partial_i\Psi
\end{aligned} \tag{A.9}$$

where we have not used the background and first order equations for simplification yet. Similarly, the energy momentum tensor is given by:

$$\begin{aligned}
T_{ij}^{(2)} = & a^2\left(\delta_{ij}\left[\frac{1}{2}P^{(2)} - 2c_s^2\delta\rho\Psi - w\rho\Psi^{(2)}\right] + 2c_s^2\delta\rho h_{ij} + (1+w)\rho\partial_iv\partial_jv\right. \\
& \left. + w\rho h_{ij}^{(2)}\right).
\end{aligned} \tag{A.10}$$

B Fourier space conventions

In this Appendix we present our choice of conventions in Fourier space in which we carry out our work.

A scalar quantity, $S(\mathbf{x}, \eta)$, can be expressed as a Fourier integral

$$S(\mathbf{x}, \eta) = \frac{1}{2\pi^{\frac{3}{2}}} \int d^3\mathbf{k} S(\mathbf{k}, \eta) e^{i\mathbf{k}\cdot\mathbf{x}}. \tag{B.1}$$

Similarly, a symmetric transverse-traceless tensor, $T_{ab}(\mathbf{x}, \eta)$, in real space can be expressed as a Fourier integral

$$T_{ab}(\mathbf{x}, \eta) = \frac{1}{2\pi^{\frac{3}{2}}} \int d^3\mathbf{k} \{T(\mathbf{k}, \eta)q_{ab}(\mathbf{k}) + \bar{T}(\mathbf{k}, \eta)\bar{q}_{ab}(\mathbf{k})\} e^{i\mathbf{k}\cdot\mathbf{x}}, \tag{B.2}$$

where we note that the two polarizations decouple. The tensor basis is given in terms of two time-independent polarization tensors $q_{ab}(\mathbf{k})$ and $\bar{q}_{ab}(\mathbf{k})$ which, respectively, are the ‘plus’ and ‘cross’ polarizations of a gravitational wave. These tensors can be expressed in terms of

vectors that are orthogonal to the direction of propagation of the gravitational wave, \mathbf{k} :

$$\begin{aligned} q_{ab}^+(\mathbf{k}) &= \frac{1}{\sqrt{2}} (e_a(\mathbf{k})e_b(\mathbf{k}) - \bar{e}_a(\mathbf{k})\bar{e}_b(\mathbf{k})) \\ q_{ab}^\times(\mathbf{k}) &= \frac{1}{\sqrt{2}} (e_a(\mathbf{k})\bar{e}_b(\mathbf{k}) + \bar{e}_a(\mathbf{k})e_b(\mathbf{k})) \end{aligned} \quad (\text{B.3})$$

The basis vectors obey:

$$e_a e^a = \bar{e}_a \bar{e}^a = 1, \quad e_a \bar{e}^a = 0, \quad e_a k^a = \bar{e}_a k^a = 0, \quad (\text{B.4})$$

and hence the symmetric tensor basis satisfies ($\lambda = +, \times$):

$$q_{ab}^\lambda(\mathbf{k})\delta^{ab} = 0, \quad q_{ab}^\lambda(\mathbf{k})k^a = 0, \quad q_{ab}^\lambda(\mathbf{k})q^{ab,\lambda'}(\mathbf{k}) = \delta^{\lambda\lambda'}. \quad (\text{B.5})$$

Additionally $q_{ij}^\lambda(\mathbf{k})$ can be taken to be real, so that: $q_{ij}^\lambda(\mathbf{k}) = q_{ij}^\lambda(-\mathbf{k})$.

It is useful to parameterize the vectors and basis tensors in spherical coordinates, since FLRW spacetime is spherically symmetric. The wave-vector \mathbf{k} is expressed as:

$$\mathbf{k} = k (\sin \theta_k \cos \phi_k, \sin \theta_k \sin \phi_k, \cos \theta_k) , \quad (\text{B.6})$$

in the (k, θ, ϕ) coordinate system, with $\phi \in [0; 2\pi[$ and $\theta \in [0; \pi]$. We can construct two orthonormal vectors in the subspace perpendicular to \mathbf{k} :

$$\begin{aligned} \mathbf{e}(\mathbf{k}) &= (\cos \theta_k \cos \phi_k, \cos \theta_k \sin \phi_k, -\sin \theta_k) , \\ \bar{\mathbf{e}}(\mathbf{k}) &= (-\sin \phi_k, \cos \phi_k, 0) . \end{aligned} \quad (\text{B.7})$$

Furthermore, due to isotropy we have the freedom to align \mathbf{k} with the z -axis, therefore $\theta_k = \phi_k = 0$. Similarly, for the the vector \mathbf{p} :

$$\mathbf{p} = p (\sin \theta_p \cos \phi_p, \sin \theta_p \sin \phi_p, \cos \theta_p) , \quad (\text{B.8})$$

from which we get the important result:

$$|\mathbf{k} - \mathbf{p}|^2 = k^2 + p^2 - 2kp \cos \theta_p . \quad (\text{B.9})$$

C Polarization functions

In this Appendix we show that the convolution integral is invariant under the switching of the two variables of the convolution and provide the results for the polarization function integrals in the azimuthal direction.

C.1 Convolution symmetry in the tensor-tensor sector

As stated previously, due to the nature of the second order computation (i.e. a convolution) there is a symmetry between \mathbf{p} and $\mathbf{k} - \mathbf{p}$ that can be exploited to simplify computations when extracting the power spectrum for the scalar-scalar and tensor-tensor induced waves. This has been shown in Ref. [43] and for the case of scalar-scalar induced waves in Ref. [40]. Here we extend this reasoning for convoluted terms quadratic in tensor perturbations.

When we substitute Eq. (3.12) into Eq. (3.11), we use the fact that integrating over $\delta(\mathbf{p} + \mathbf{p}')$ or $\delta(\mathbf{p} + \mathbf{k}' - \mathbf{p}')$ is the same since there is a symmetry originating from the convolution. Consider a term that appears in Eq. (2.14), for example:

$$\int d^3\mathbf{p} q_\lambda^{ab}(\mathbf{k}) q_a^{m,\lambda_1}(\mathbf{k} - \mathbf{p}) q_{bm}^{\lambda_2}(\mathbf{p}) f(p) f(k - p) \quad (\text{C.1})$$

We want to show that the integral is unchanged by switching \mathbf{p} and $\mathbf{k} - \mathbf{p}$. Let us consider the change of variable $\tilde{\mathbf{p}} = \mathbf{k} - \mathbf{p}$, then the above changes to:

$$\int d^3\tilde{\mathbf{p}} q_\lambda^{ab}(\mathbf{k}) q_a^{m,\lambda_1}(\tilde{\mathbf{p}}) q_{bm}^{\lambda_2}(\mathbf{k} - \tilde{\mathbf{p}}) f(k - \tilde{p}) f(\tilde{p}) \quad (\text{C.2})$$

We have the freedom to relabel $a \leftrightarrow b$ and using the fact that $q^{ab}(\mathbf{k})$ is symmetric we have:

$$\int d^3\tilde{\mathbf{p}} q_\lambda^{ab}(\mathbf{k}) q_b^{m,\lambda_1}(\tilde{\mathbf{p}}) q_{am}^{\lambda_2}(\mathbf{k} - \tilde{\mathbf{p}}) f(k - \tilde{p}) f(\tilde{p}) \quad (\text{C.3})$$

Finally, remembering that there is an implicit sum over λ_1 and λ_2 (i.e. they are just labels), we can relabel them, so that:

$$\int d^3\tilde{\mathbf{p}} q_\lambda^{ab}(\mathbf{k}) q_a^{m,\lambda_1}(\mathbf{k} - \tilde{\mathbf{p}}) q_{bm}^{\lambda_2}(\tilde{\mathbf{p}}) f(\tilde{p}) f(k - \tilde{p}) \quad (\text{C.4})$$

This reasoning can be extended to all the tensor-tensor terms that appear in Eq. (2.15).

C.2 Integral evaluations of the polarization functions

After switching to spherical coordinates, the polarization functions in Eq. (2.15) are evaluated to be:

$$q^{\lambda,ss}(k, p) = \begin{cases} \frac{1}{\sqrt{2}} p^2 \sin^2 \theta \cos 2\phi & \lambda = + \\ \frac{1}{\sqrt{2}} p^2 \sin^2 \theta \sin 2\phi & \lambda = \times \end{cases} \quad (\text{C.5})$$

$$q_1^{\lambda,tt}(k, p) = \begin{cases} \frac{1}{\sqrt{2}} p^2 \sin^2 \theta \cos 2\phi & \lambda = + \\ \frac{1}{\sqrt{2}} p^2 \sin^2 \theta \sin 2\phi & \lambda = \times \end{cases} \quad (\text{C.6})$$

$$q_2^{\lambda,tt}(k, p) = \begin{cases} -\frac{1}{\sqrt{2}} \sin^2 \theta \cos 2\phi & \lambda = + \\ -\frac{1}{\sqrt{2}} \sin^2 \theta \sin 2\phi & \lambda = \times \end{cases} \quad (\text{C.7})$$

$$q^{\lambda,st}(k, p) = \begin{cases} \frac{1}{2} ((1 + \cos \theta_p^2)(\cos \phi_p^2 - \sin \phi_p^2) - 4 \cos \theta_p \cos \phi_p \sin \phi_p) & \lambda = + \\ \cos \theta_p \cos 2\phi_p + \cos \phi_p \sin \phi_p (1 + \cos \theta_p^2) & \lambda = \times \end{cases} \quad (\text{C.8})$$

The expressions that contribute to the power spectrum are listed below (once integrated over the azimuthal angle). For the pure scalar part:

$$\begin{aligned} \int_0^{2\pi} q^{\lambda,ss} q^{\lambda',ss} &= \frac{1}{2} p^4 \pi \sin^4 \theta_p \delta^{\lambda\lambda'} \\ &= \frac{1}{2} k^4 \pi v^4 \left(1 - \frac{(1 + v^2 - u^2)^2}{4v^2} \right)^2 \delta^{\lambda\lambda'}, \end{aligned} \quad (\text{C.9})$$

where in the last equality we used:

$$\sin^2 \theta_p = 1 - \frac{(1 + v^2 - u^2)^2}{4v^2} = 1 - \cos^2 \theta_p . \quad (\text{C.10})$$

For the pure tensor part, the resulting expressions are:

$$\int_0^{2\pi} q_1^{\lambda,tt} q_1^{\lambda',tt} = \frac{1}{2} k^4 \pi v^4 \left(1 - \frac{(1 + v^2 - u^2)^2}{4v^2} \right)^2 \delta^{\lambda\lambda'} , \quad (\text{C.11})$$

$$\int_0^{2\pi} q_1^{\lambda,tt} q_2^{\lambda',tt} = -\frac{1}{2} \pi k^2 v^2 \left(1 - \frac{(v^2 - u^2 + 1)^2}{4v^2} \right)^2 \delta^{\lambda\lambda'} , \quad (\text{C.12})$$

$$\int_0^{2\pi} q_2^{\lambda,tt} q_2^{\lambda',tt} = \frac{1}{2} \pi \left(1 - \frac{(v^2 - u^2 + 1)^2}{4v^2} \right)^2 \delta^{\lambda\lambda'} . \quad (\text{C.13})$$

Finally the cross term contributes as:

$$\begin{aligned} \int_0^{2\pi} q^{\lambda,st} q^{\lambda',st} &= \frac{\pi}{64v^4} \left((u^2 - 1)^4 - 4v^2(u^2 - 7)(u^2 - 1)^2 + 2v^4(3u^4 - 30u^2 + 35) + v^8 \right. \\ &\quad \left. - 4v^6(u^2 - 7) \right) \delta^{\lambda\lambda'} \\ &\equiv \pi M_{st}(v, u) \delta^{\lambda\lambda'} . \end{aligned} \quad (\text{C.14})$$

D Evaluation of kernels

D.1 Definition of the functions

In Eq. (2.16) we defined several functions. Here they are:

$$\begin{aligned} f^{ss}(\eta, k, |\mathbf{k} - \mathbf{p}|) &= \frac{2}{3(1+w)} \left[\left(T_\Psi(\eta|\mathbf{k} - \mathbf{p}|) + \frac{T'_\Psi(\eta|\mathbf{k} - \mathbf{p}|)}{\mathcal{H}} \right) \left(T_\Psi(\eta p) + \frac{T'_\Psi(\eta p)}{\mathcal{H}} \right) \right] \\ &\quad + T_\Psi(\eta|\mathbf{k} - \mathbf{p}|) T_\Psi(\eta p) , \end{aligned} \quad (\text{D.1})$$

Tensor terms:

$$f_1^{tt}(\eta, k, |\mathbf{k} - \mathbf{p}|) = T_E(\eta|\mathbf{k} - \mathbf{p}|) T_h(\eta p) , \quad (\text{D.2a})$$

$$f_2^{tt}(\eta, k, |\mathbf{k} - \mathbf{p}|) = T'_E(\eta|\mathbf{k} - \mathbf{p}|) T'_E(\eta p) , \quad (\text{D.2b})$$

Cross term:

$$\begin{aligned} f^{st}(\eta p, c_s \eta |\mathbf{k} - \mathbf{p}|) &= -2p^2 T_h(\eta p) T_\Psi(c_s \eta |\mathbf{k} - \mathbf{p}|) - 2(k - p) p T_h(\eta p) T_\Psi(c_s \eta |\mathbf{k} - \mathbf{p}|) \\ &\quad + \mathcal{H}(1 + 3c_s^2) T_h(\eta p) T'_\Psi(c_s \eta |\mathbf{k} - \mathbf{p}|) - (k - p)^2 (1 - c_s^2) T_h(\eta p) \\ &\quad \times T_\Psi(c_s \eta |\mathbf{k} - \mathbf{p}|) . \end{aligned} \quad (\text{D.3})$$

We can write everything in terms of the variables v and u in Eq. (3.5). The scalar-scalar terms:

$$f^{ss}(x, u, v, c_s) = \frac{2}{3(1+w)} \left[\left(T_{\Psi}(c_s xv) + x \frac{\partial T_{\Psi}(c_s xv)}{\partial x} \right) \left(T_{\Psi}(c_s xu) + x \frac{\partial T_{\Psi}(c_s xu)}{\partial x} \right) \right] + T_{\Psi}(c_s xv) T_{\Psi}(c_s xu) , \quad (\text{D.4})$$

Tensor-tensor terms:

$$f_1^{tt}(x, v, u) = T_h(xv) T_h(xu) , \quad (\text{D.5a})$$

$$f_2^{tt}(x, v, u) = k^2 \frac{\partial T_h(xv)}{\partial x} \frac{\partial T_h(xu)}{\partial x} , \quad (\text{D.5b})$$

and finally the cross term:

$$f^{st}(x, u, v, c_s) = -2v^2 k^2 T_h(xv) T_{\Psi}(c_s xu) - 2vuk^2 T_h(xv) T_{\Psi}(c_s xu) + (1 + 3c_s^2) \frac{k^2}{x} T_h(xv) \frac{\partial T_{\Psi}(c_s xu)}{\partial x} - u^2 k^2 (1 - c_s^2) T_h(xv) T_{\Psi}(c_s xu) . \quad (\text{D.6})$$

D.2 Kernel results

All the Kernels presented in Eq. (3.15) and Eq. (3.21) can be evaluated analytically and our presented below. These are trigonometric integrals, so it is useful to recall the following definitions:

$$Si(z) = \int_0^z \frac{\sin t}{t} dt \quad Ci(z) = - \int_z^{\infty} \frac{\cos t}{t} dt$$

and their finite limits: $\lim_{x \rightarrow \infty} Si(z) = \pm \frac{\pi}{2}$ and $\lim_{x \rightarrow \infty} Ci(z) = 0$.

First we give the result from [41] for the scalar-scalar Kernel, $c_s = 1/\sqrt{3}$:

$$I^{ss}(v, u, x \rightarrow \infty) = \frac{3(u^2 + v^2 - 3)}{4u^3 v^3 x} \left[\sin x \left(-4uv + (u^2 + v^2 - 3) \log \left| \frac{3 - (u+v)^2}{3 - (u-v)^2} \right| \right) - \pi \cos x (u^2 + v^2 - 3) \Theta(v + u - \sqrt{3}) \right] . \quad (\text{D.7})$$

The evaluation of the tensor-tensor kernels are presented below. For concreteness, we show the steps for $\mathcal{I}_{c,1}^{tt}(x, v, u)$ and $\mathcal{I}_{s,1}^{tt}(x, v, u)$ in Eq. (3.15):

$$\mathcal{I}_{c,1}^{tt}(x, v, u) = -\frac{1}{4uv} \left[\text{Si}((u-v+1)x) + \text{Si}((-u+v+1)x) + \text{Si}((u+v-1)x) - \text{Si}((u+v+1)x) \right] , \quad (\text{D.8})$$

$$\mathcal{I}_{s,1}^{tt}(x, v, u) = \frac{1}{4uv} \left[\text{Ci}(|u-v-1|x) + \text{Ci}(|u-v+1|x) - \text{Ci}(|u+v+1|x) - \text{Ci}(|u+v-1|x) - \log \left| \frac{(u-v-1)(u-v+1)}{(u+v+1)(u+v-1)} \right| \right] . \quad (\text{D.9})$$

Since we are interested in modes that are deep inside the horizon we take the limit where $k\eta \gg 1$, or equivalently sending $x \rightarrow \infty$.

$$\mathcal{I}_{c,1}^{tt}(x \rightarrow \infty, v, u) = -\frac{\pi}{4uv} \Theta(u + v - 1) , \quad (\text{D.10})$$

$$\mathcal{I}_{s,1}^{tt}(x \rightarrow \infty, v, u) = \frac{1}{4uv} \log \left| \frac{1 - (u + v)^2}{1 - (u - v)^2} \right| . \quad (\text{D.11})$$

Similarly for $\mathcal{I}_{c,2}^{tt}(x, v, u)$ and $\mathcal{I}_{s,2}^{tt}(x, v, u)$:

$$\begin{aligned} \mathcal{I}_{c,2}^{tt}(x, v, u) = & \frac{k^2}{2uvx^2} [\sin x \sin ux \sin vx] + \frac{4k^2}{8uvx} [-v \sin x \sin ux \cos vx \\ & + \cos x \sin ux \sin vx - u \sin x \cos ux \sin vx] - \frac{k^2 (u^2 + v^2 - 1)}{8uv} \left[\right. \\ & \text{Si}((u - v + 1)x) + \text{Si}((-u + v + 1)x) - \text{Si}((u + v + 1)x) \\ & \left. - \text{Si}(-ux - vx + x) \right] , \end{aligned} \quad (\text{D.12})$$

$$\mathcal{I}_{c,2}^{tt}(x \rightarrow \infty, v, u) = -\frac{\pi k^2 (u^2 + v^2 - 1)}{8uv} \Theta(u + v - 1) . \quad (\text{D.13})$$

and

$$\begin{aligned} \mathcal{I}_{s,2}^{tt}(x, v, u) = & \frac{k^2}{2uvx^2} (\cos x \sin ux \sin vx) + \frac{k^2}{2uvx} (\sin x \sin ux \sin vx + v \cos x \sin ux \cos vx \\ & + u \cos x \cos ux \sin vx) - \frac{k^2}{8uv} (u^2 + v^2 - 1) \left(\text{Ci}(|u + v - 1|x) + \text{Ci}(|u + v + 1|x) \right. \\ & \left. - \text{Ci}(|u - v - 1|x) - \text{Ci}(|u - v + 1|x) + \log \left| \frac{(u - v - 1)(u - v + 1)}{(u + v - 1)(u + v + 1)} \right| \right) \end{aligned} \quad (\text{D.14})$$

$$\mathcal{I}_{s,2}^{tt}(x \rightarrow \infty, v, u) = \frac{k^2}{8uv} \left((u^2 + v^2 - 1) \log \left| \frac{1 - (u + v)^2}{1 - (u - v)^2} \right| - 4vu \right) . \quad (\text{D.15})$$

Below we present the results for the scalar-tensor kernels, which is the evaluation of Eq. (3.21). These expressions are much more involved than the tensor-tensor kernels, therefore we display only the part that will contribute to the final expression, i.e. the limit where $x \rightarrow \infty$. $\mathcal{I}_c^{st}(x \rightarrow \infty, v, u)$ reads:

$$\mathcal{I}_c^{st}(x \rightarrow \infty, v, u) = \frac{3\pi k^2}{32u^3 v c_s^3} (1 + c_s u - v)(-1 + c_s u + v) i_{-}^{st}(v, u) \Theta(v + u c_s - 1), \quad (\text{D.16})$$

where for compactness we defined:

$$i_{\pm}^{st}(v, u) = -1 + 4u^2 - 3c_s^2(u^2 + (v \pm 1)^2 - c_s^2 u^2) + 8uv + v(\mp 2 + 7v) . \quad (\text{D.17})$$

and $\mathcal{I}_s^{st}(x \rightarrow \infty, v, u)$:

$$\begin{aligned} \mathcal{I}_s^{st}(x \rightarrow \infty, v, u) = & \frac{3k^2}{32c_s^3 u^3 v} \left(i_{+}^{st}(v, u) \log \left| \frac{c_s u - v - 1}{c_s u + v + 1} \right| (c_s u - v - 1)(c_s u + v + 1) \right. \\ & + i_{-}^{st}(v, u) \log \left| \frac{c_s u - v + 1}{c_s u + v - 1} \right| (c_s u - v + 1)(c_s u + v - 1) - \frac{4}{9} c_s u v \left[-9 \right. \\ & \left. \left. + 12u^2 + 15c_s^4 u^2 + 3v(8u + 7v) - c_s^2(7u^2 + 3(9 + v^2)) \right] \right) . \end{aligned} \quad (\text{D.18})$$

References

- [1] B. P. Abbott *et al.* [LIGO Scientific and Virgo], “Observation of Gravitational Waves from a Binary Black Hole Merger,” *Phys. Rev. Lett.* **116** (2016) no.6, 061102
doi:10.1103/PhysRevLett.116.061102 [arXiv:1602.03837 [gr-qc]].
- [2] G. Agazie *et al.* [NANOGrav], “The NANOGrav 15 yr Data Set: Evidence for a Gravitational-wave Background,” *Astrophys. J. Lett.* **951** (2023) no.1, L8
doi:10.3847/2041-8213/acdac6 [arXiv:2306.16213 [astro-ph.HE]].
- [3] J. Antoniadis, S. Babak, A. S. Bak Nielsen, C. G. Bassa, A. Berthureau, M. Bonetti, E. Bortolas, P. R. Brook, M. Burgay and R. N. Caballero, *et al.* “The second data release from the European Pulsar Timing Array I. The dataset and timing analysis,”
doi:10.1051/0004-6361/202346841 [arXiv:2306.16224 [astro-ph.HE]].
- [4] J. Antoniadis, P. Arumugam, S. Arumugam, S. Babak, M. Bagchi, A. S. B. Nielsen, C. G. Bassa, A. Bathula, A. Berthureau and M. Bonetti, *et al.* “The second data release from the European Pulsar Timing Array III. Search for gravitational wave signals,”
[arXiv:2306.16214 [astro-ph.HE]].
- [5] J. Antoniadis, P. Arumugam, S. Arumugam, P. Auclair, S. Babak, M. Bagchi, A. S. Bak Nielsen, E. Barausse, C. G. Bassa and A. Bathula, *et al.* “The second data release from the European Pulsar Timing Array: V. Implications for massive black holes, dark matter and the early Universe,” [arXiv:2306.16227 [astro-ph.CO]].
- [6] H. Xu, S. Chen, Y. Guo, J. Jiang, B. Wang, J. Xu, Z. Xue, R. N. Caballero, J. Yuan and Y. Xu, *et al.* “Searching for the Nano-Hertz Stochastic Gravitational Wave Background with the Chinese Pulsar Timing Array Data Release I,” *Res. Astron. Astrophys.* **23** (2023) no.7, 075024 doi:10.1088/1674-4527/acdfa5 [arXiv:2306.16216 [astro-ph.HE]].
- [7] D. J. Reardon, A. Zic, R. M. Shannon, G. B. Hobbs, M. Bailes, V. Di Marco, A. Kapur, A. F. Rogers, E. Thrane and J. Askew, *et al.* “Search for an Isotropic Gravitational-wave Background with the Parkes Pulsar Timing Array,” *Astrophys. J. Lett.* **951** (2023) no.1, L6
doi:10.3847/2041-8213/acdd02 [arXiv:2306.16215 [astro-ph.HE]].
- [8] A. Zic, D. J. Reardon, A. Kapur, G. Hobbs, R. Mandow, M. Curyło, R. M. Shannon, J. Askew, M. Bailes and N. D. R. Bhat, *et al.* “The Parkes Pulsar Timing Array Third Data Release,”
[arXiv:2306.16230 [astro-ph.HE]].
- [9] A. Afzal *et al.* [NANOGrav], “The NANOGrav 15 yr Data Set: Search for Signals from New Physics,” *Astrophys. J. Lett.* **951** (2023) no.1, L11 doi:10.3847/2041-8213/acdc91
[arXiv:2306.16219 [astro-ph.HE]].
- [10] A. R. Liddle and D. H. Lyth, “Cosmological inflation and large scale structure,”
doi:10.1017/CBO9781139175180
- [11] K. Tomita, “Non-Linear Theory of Gravitational Instability in the Expanding Universe”,
Progress of Theoretical Physics **37** (1967) 831
[https://academic.oup.com/ptp/article-pdf/37/5/831/5234391/37-5-831.pdf]
- [12] N. Aghanim *et al.* [Planck], “Planck 2018 results. VI. Cosmological parameters,” *Astron. Astrophys.* **641** (2020), A6 [erratum: *Astron. Astrophys.* **652** (2021), C4]
doi:10.1051/0004-6361/201833910 [arXiv:1807.06209 [astro-ph.CO]].
- [13] S. Matarrese, O. Pantano and D. Saez, “A General relativistic approach to the nonlinear evolution of collisionless matter,” *Phys. Rev. D* **47** (1993), 1311-1323
doi:10.1103/PhysRevD.47.1311
- [14] S. Matarrese, O. Pantano and D. Saez, “General relativistic dynamics of irrotational dust: Cosmological implications,” *Phys. Rev. Lett.* **72** (1994), 320-323
doi:10.1103/PhysRevLett.72.320 [arXiv:astro-ph/9310036 [astro-ph]].

- [15] S. Matarrese, S. Mollerach and M. Bruni, “Second order perturbations of the Einstein-de Sitter universe,” *Phys. Rev. D* **58** (1998), 043504 doi:10.1103/PhysRevD.58.043504 [arXiv:astro-ph/9707278 [astro-ph]].
- [16] K. N. Ananda, C. Clarkson and D. Wands, “The Cosmological gravitational wave background from primordial density perturbations,” *Phys. Rev. D* **75** (2007), 123518 doi:10.1103/PhysRevD.75.123518 [arXiv:gr-qc/0612013 [gr-qc]].
- [17] D. Baumann, P. J. Steinhardt, K. Takahashi and K. Ichiki, “Gravitational Wave Spectrum Induced by Primordial Scalar Perturbations,” *Phys. Rev. D* **76** (2007), 084019 doi:10.1103/PhysRevD.76.084019 [arXiv:hep-th/0703290 [hep-th]].
- [18] G. Domènech, “Scalar Induced Gravitational Waves Review,” *Universe* **7** (2021) no.11, 398 doi:10.3390/universe7110398 [arXiv:2109.01398 [gr-qc]].
- [19] G. Domènech, C. Lin and M. Sasaki, “Gravitational wave constraints on the primordial black hole dominated early universe,” *JCAP* **04** (2021), 062 [erratum: *JCAP* **11** (2021), E01] doi:10.1088/1475-7516/2021/11/E01 [arXiv:2012.08151 [gr-qc]].
- [20] Z. Chang, X. Zhang and J. Z. Zhou, “Gravitational waves from primordial scalar and tensor perturbations,” [arXiv:2209.07693 [astro-ph.CO]].
- [21] W. H. Kinney, “A Hamilton-Jacobi approach to nonslow roll inflation,” *Phys. Rev. D* **56** (1997), 2002-2009 doi:10.1103/PhysRevD.56.2002 [arXiv:hep-ph/9702427 [hep-ph]].
- [22] J. Garcia-Bellido and E. Ruiz Morales, “Primordial black holes from single field models of inflation,” *Phys. Dark Univ.* **18** (2017), 47-54 doi:10.1016/j.dark.2017.09.007 [arXiv:1702.03901 [astro-ph.CO]].
- [23] L. Iacconi, H. Assadullahi, M. Fasiello and D. Wands, “Revisiting small-scale fluctuations in α -attractor models of inflation,” *JCAP* **06** (2022) no.06, 007 doi:10.1088/1475-7516/2022/06/007 [arXiv:2112.05092 [astro-ph.CO]].
- [24] H. Motohashi and W. Hu, “Primordial Black Holes and Slow-Roll Violation,” *Phys. Rev. D* **96** (2017) no.6, 063503 doi:10.1103/PhysRevD.96.063503 [arXiv:1706.06784 [astro-ph.CO]].
- [25] J. Fumagalli, S. Renaux-Petel, J. W. Ronayne and L. T. Witkowski, “Turning in the landscape: A new mechanism for generating primordial black holes,” *Phys. Lett. B* **841** (2023), 137921 doi:10.1016/j.physletb.2023.137921 [arXiv:2004.08369 [hep-th]].
- [26] G. A. Palma, S. Sypsas and C. Zenteno, “Seeding primordial black holes in multifield inflation,” *Phys. Rev. Lett.* **125** (2020) no.12, 121301 doi:10.1103/PhysRevLett.125.121301 [arXiv:2004.06106 [astro-ph.CO]].
- [27] M. Braglia, D. K. Hazra, F. Finelli, G. F. Smoot, L. Sriramkumar and A. A. Starobinsky, “Generating PBHs and small-scale GWs in two-field models of inflation,” *JCAP* **08** (2020), 001 doi:10.1088/1475-7516/2020/08/001 [arXiv:2005.02895 [astro-ph.CO]].
- [28] N. Barnaby, E. Pajer and M. Peloso, “Gauge Field Production in Axion Inflation: Consequences for Monodromy, non-Gaussianity in the CMB, and Gravitational Waves at Interferometers,” *Phys. Rev. D* **85** (2012), 023525 doi:10.1103/PhysRevD.85.023525 [arXiv:1110.3327 [astro-ph.CO]].
- [29] B. Thorne, T. Fujita, M. Hazumi, N. Katayama, E. Komatsu and M. Shiraishi, “Finding the chiral gravitational wave background of an axion-SU(2) inflationary model using CMB observations and laser interferometers,” *Phys. Rev. D* **97** (2018) no.4, 043506 doi:10.1103/PhysRevD.97.043506 [arXiv:1707.03240 [astro-ph.CO]].
- [30] E. Dimastrogiovanni, M. Fasiello and T. Fujita, “Primordial Gravitational Waves from Axion-Gauge Fields Dynamics,” *JCAP* **01** (2017), 019 doi:10.1088/1475-7516/2017/01/019 [arXiv:1608.04216 [astro-ph.CO]].

- [31] N. Bartolo, C. Caprini, V. Domcke, D. G. Figueroa, J. Garcia-Bellido, M. C. Guzzetti, M. Liguori, S. Matarrese, M. Peloso and A. Petiteau, *et al.* “Science with the space-based interferometer LISA. IV: Probing inflation with gravitational waves,” *JCAP* **12** (2016), 026 doi:10.1088/1475-7516/2016/12/026 [arXiv:1610.06481 [astro-ph.CO]].
- [32] S. Kawamura, M. Ando, N. Seto, S. Sato, M. Musha, I. Kawano, J. Yokoyama, T. Tanaka, K. Ioka and T. Akutsu, *et al.* “Current status of space gravitational wave antenna DECIGO and B-DECIGO,” *PTEP* **2021** (2021) no.5, 05A105 doi:10.1093/ptep/ptab019 [arXiv:2006.13545 [gr-qc]].
- [33] S. Hild, M. Abernathy, F. Acernese, P. Amaro-Seoane, N. Andersson, K. Arun, F. Barone, B. Barr, M. Barsuglia and M. Beker, *et al.* “Sensitivity Studies for Third-Generation Gravitational Wave Observatories,” *Class. Quant. Grav.* **28** (2011), 094013 doi:10.1088/0264-9381/28/9/094013 [arXiv:1012.0908 [gr-qc]].
- [34] C. Yuan, Z. C. Chen and Q. G. Huang, “Log-dependent slope of scalar induced gravitational waves in the infrared regions,” *Phys. Rev. D* **101** (2020) no.4, 043019 doi:10.1103/PhysRevD.101.043019 [arXiv:1910.09099 [astro-ph.CO]].
- [35] C. J. Moore, R. H. Cole and C. P. L. Berry, “Gravitational-wave sensitivity curves,” *Class. Quant. Grav.* **32** (2015) no.1, 015014 doi:10.1088/0264-9381/32/1/015014 [arXiv:1408.0740 [gr-qc]].
- [36] J. O. Gong, “Analytic Integral Solutions for Induced Gravitational Waves,” *Astrophys. J.* **925** (2022) no.1, 102 doi:10.3847/1538-4357/ac3a6c [arXiv:1909.12708 [gr-qc]].
- [37] P. Bari, N. Bartolo, G. Domènech and S. Matarrese, “Gravitational waves induced by scalar-tensor mixing,” [arXiv:2307.05404 [astro-ph.CO]].
- [38] Y. H. Yu and S. Wang, “Primordial Gravitational Waves Assisted by Cosmological Scalar Perturbations,” [arXiv:2303.03897 [astro-ph.CO]].
- [39] P. Peter and J. P. Uzan, “Primordial Cosmology,” Oxford University Press, 2013, ISBN 978-0-19-966515-0, 978-0-19-920991-0
- [40] J. R. Espinosa, D. Racco and A. Riotto, “A Cosmological Signature of the SM Higgs Instability: Gravitational Waves,” *JCAP* **09** (2018), 012 doi:10.1088/1475-7516/2018/09/012 [arXiv:1804.07732 [hep-ph]].
- [41] K. Kohri and T. Terada, “Semianalytic calculation of gravitational wave spectrum nonlinearly induced from primordial curvature perturbations,” *Phys. Rev. D* **97** (2018) no.12, 123532 doi:10.1103/PhysRevD.97.123532 [arXiv:1804.08577 [gr-qc]].
- [42] K. A. Malik and D. Wands, “Cosmological perturbations,” *Phys. Rept.* **475** (2009), 1-51 doi:10.1016/j.physrep.2009.03.001 [arXiv:0809.4944 [astro-ph]].
- [43] K. A. Malik, “A not so short note on the Klein-Gordon equation at second order,” *JCAP* **03** (2007), 004 doi:10.1088/1475-7516/2007/03/004 [arXiv:astro-ph/0610864 [astro-ph]].
- [44] S. Pi and M. Sasaki, “Gravitational Waves Induced by Scalar Perturbations with a Lognormal Peak,” *JCAP* **09** (2020), 037 doi:10.1088/1475-7516/2020/09/037 [arXiv:2005.12306 [gr-qc]].
- [45] B. S. Sathyaprakash and B. F. Schutz, “Physics, Astrophysics and Cosmology with Gravitational Waves,” *Living Rev. Rel.* **12** (2009), 2 doi:10.12942/lrr-2009-2 [arXiv:0903.0338 [gr-qc]].
- [46] P. Auclair *et al.* [LISA Cosmology Working Group], “Cosmology with the Laser Interferometer Space Antenna,” *Living Rev. Rel.* **26** (2023) no.1, 5 doi:10.1007/s41114-023-00045-2 [arXiv:2204.05434 [astro-ph.CO]].
- [47] Y. Akrami *et al.* [Planck], “Planck 2018 results. X. Constraints on inflation,” *Astron. Astrophys.* **641** (2020), A10 doi:10.1051/0004-6361/201833887 [arXiv:1807.06211 [astro-ph.CO]].

- [48] C. Pitrou, X. Roy and O. Umeh, “xPand: An algorithm for perturbing homogeneous cosmologies,” *Class. Quant. Grav.* **30** (2013), 165002 doi:10.1088/0264-9381/30/16/165002 [arXiv:1302.6174 [astro-ph.CO]].
- [49] C. Caprini and D. G. Figueroa, “Cosmological Backgrounds of Gravitational Waves,” *Class. Quant. Grav.* **35** (2018) no.16, 163001 doi:10.1088/1361-6382/aac608 [arXiv:1801.04268 [astro-ph.CO]].
- [50] D. J. Mulryne and J. W. Ronayne, “PyTransport: A Python package for the calculation of inflationary correlation functions,” *J. Open Source Softw.* **3** (2018) no.23, 494 doi:10.21105/joss.00494 [arXiv:1609.00381 [astro-ph.CO]].